iScience

CellPress
OPEN ACCESS

Article

Critical Network Structures and Medical Ecology Mechanisms Underlying Human Microbiome-Associated Diseases

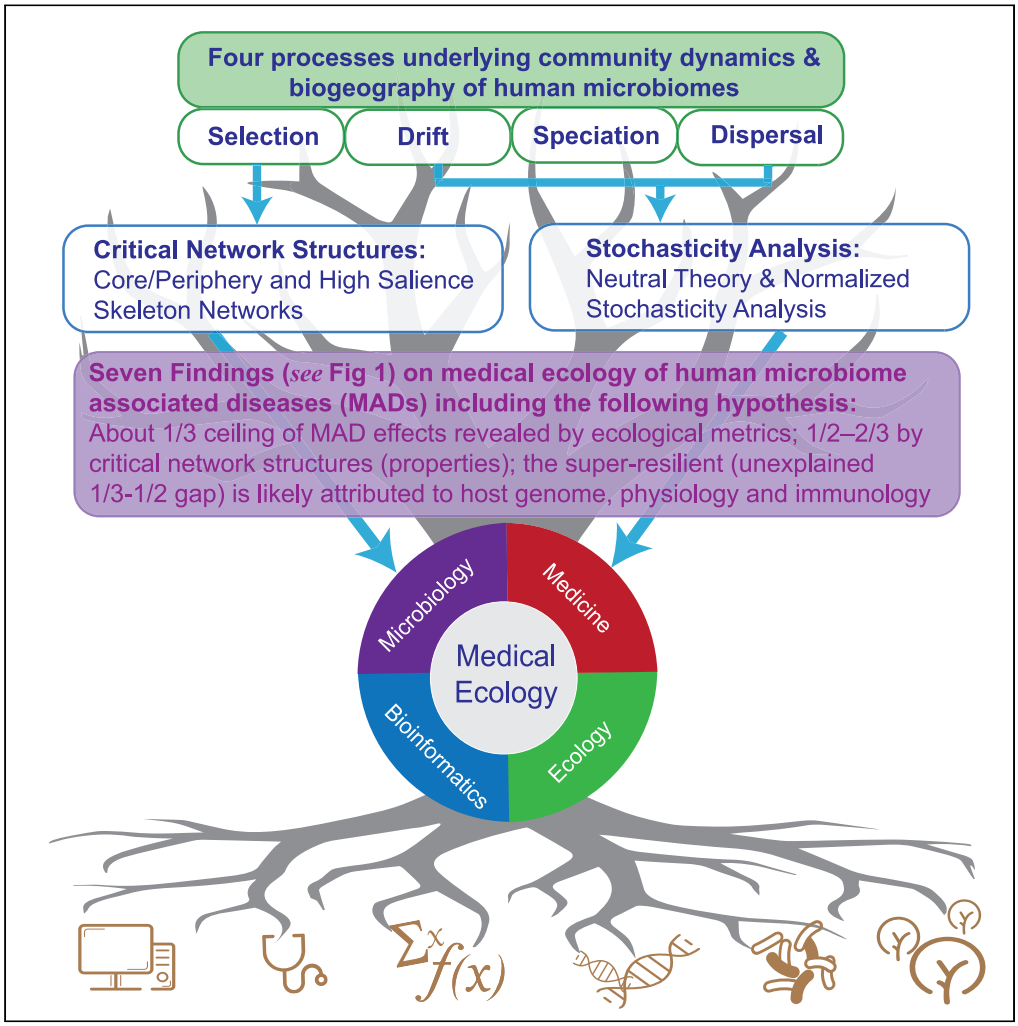

Zhanshan (Sam) Ma

ma@vandals.uidaho.edu

HIGHLIGHTS

Seven findings (mechanisms/ interpretations/ postulations) of medical ecology proposed

Critical network structures more indicative of disease effects than ecology metrics

One-third seems ceiling of diversity-disease relations, half to two-thirds of network structures

Super resilience (unexplained one-third to half gap) is likely attributed to host genome

Ma, iScience 23, 101195
June 26, 2020
https://doi.org/10.1016/j.isci.2020.101195

iScience

CellPress
OPEN ACCESS

Article

Critical Network Structures and Medical Ecology Mechanisms Underlying Human Microbiome-Associated Diseases

Zhanshan (Sam) Ma[1,2,3,*]

SUMMARY

A fundamental problem in studies on human microbiome-associated diseases (MADs) is to understand the relationships between microbiome structures and health status of hosts. For example, species diversity metrics have been routinely evaluated in virtually all studies on MADs, yet a recent meta-analysis revealed that, in only approximately one-third of the cases, diversity and diseases were related. In this study, we ask whether Hubbell's neutral theory (supplemented with the normalized stochasticity ratio [NSR]) or critical microbiome network structures may offer better alternatives. Whereas neutral theory and NSR focus on stochastic processes, we use core/periphery and high-salience skeleton networks to evaluate deterministic, asymmetrical niche effects, assuming that all species or their interactions were not "born" equal and focusing on non-neutral, critical network structures. We found that properties of critical network structures are more indicative of disease effects. Finally, seven findings (mechanisms, interpretations, and postulations) regarding medical ecology mechanisms underlying MADs were summarized.

INTRODUCTION

Despite extensive studies on the human microbiome-associated diseases (MADs) during the last decade (HMP Consortium, 2012; Integrative HMP (iHMP) Research Network Consortium, 2019), there is still little consensus on the ecological mechanism underlying the etiology of MADs. For example, the routinely computed microbiome diversity indexes (Shannon entropy, Simpson index, and species richness) and associated diversity-disease relationships (DDRs) have revealed little insights on the ecological mechanisms, not to mention insights on the disease etiology. In a recent meta-analysis of the human MADs, it was discovered that, somewhat contrary to commonly perceived intuition, there was not a consistent DDR in the majority of studied cases (approximately two-third cases)—that the species or Operational Taxonomic Unit (OTU) diversity was not related with MAD (Ma et al., 2019). This DDR in the human MADs is in strong contrast with the DDR in zoonoses, where the *dilution/amplification* hypotheses have achieved wide recognition (Johnson et al., 2013, 2015). Indeed, the disease systems and targets of diversity analysis in zoonoses and human MADs are rather different (e.g., diversity of alternative hosts or vectors in zoonoses versus diversity of microbiome). Sometimes, even more confusing is the lack of obvious pathogens and vectors in the case of human MADs, e.g., the "pathogen" of mastitis, which is related to the shift of species interactions in suppressing opportunistic pathogens (Ma et al., 2015, 2016a; Ma and Ye, 2017; Ma, 2018).

Multiple causes have contributed to the enormous challenges for the mechanistic studies on the human MADs. First, the problem itself is exceedingly complex because, the MAD, as a category of human diseases, whether the diversity change is the disease cause or consequence, may be different from case to case, and even more frustrating is that we do not yet have an answer for the cause-consequence question for many of the MADs (e.g., Castaño-Rodríguez et al., 2018; Duvallet et al., 2017; Zaneveld et al., 2017). Second, many existing studies have ignored perhaps the most important sub-system, the human immune system except for small number of studies (e.g., Zaneveld et al., 2017; Vogelzang et al., 2018; Lotter and Altfeld, 2019; Vemuri et al., 2019). Third, the etiologies of many MADs are not clear and most existing mechanistic studies were conducted with animal models (e.g., Turner, 2018). Particularly, how deeply microbiome is involved in a particular MAD can be rather different. In some cases, microbiome is likely deeply involved such as in the case of BV (bacterial vaginosis), where classic diversity-stability relationship (DSR) in

[1]Computational Biology and Medical Ecology Lab, State Key Laboratory of Genetic Resources and Evolution, Kunming Institute of Zoology, Chinese Academy of Sciences, Kunming, China

[2]Center for Excellence in Animal Evolution and Genetics, Chinese Academy of Sciences, Kunming, China

[3]Lead Contact

*Correspondence: ma@vandals.uidaho.edu

https://doi.org/10.1016/j.isci.2020.101195

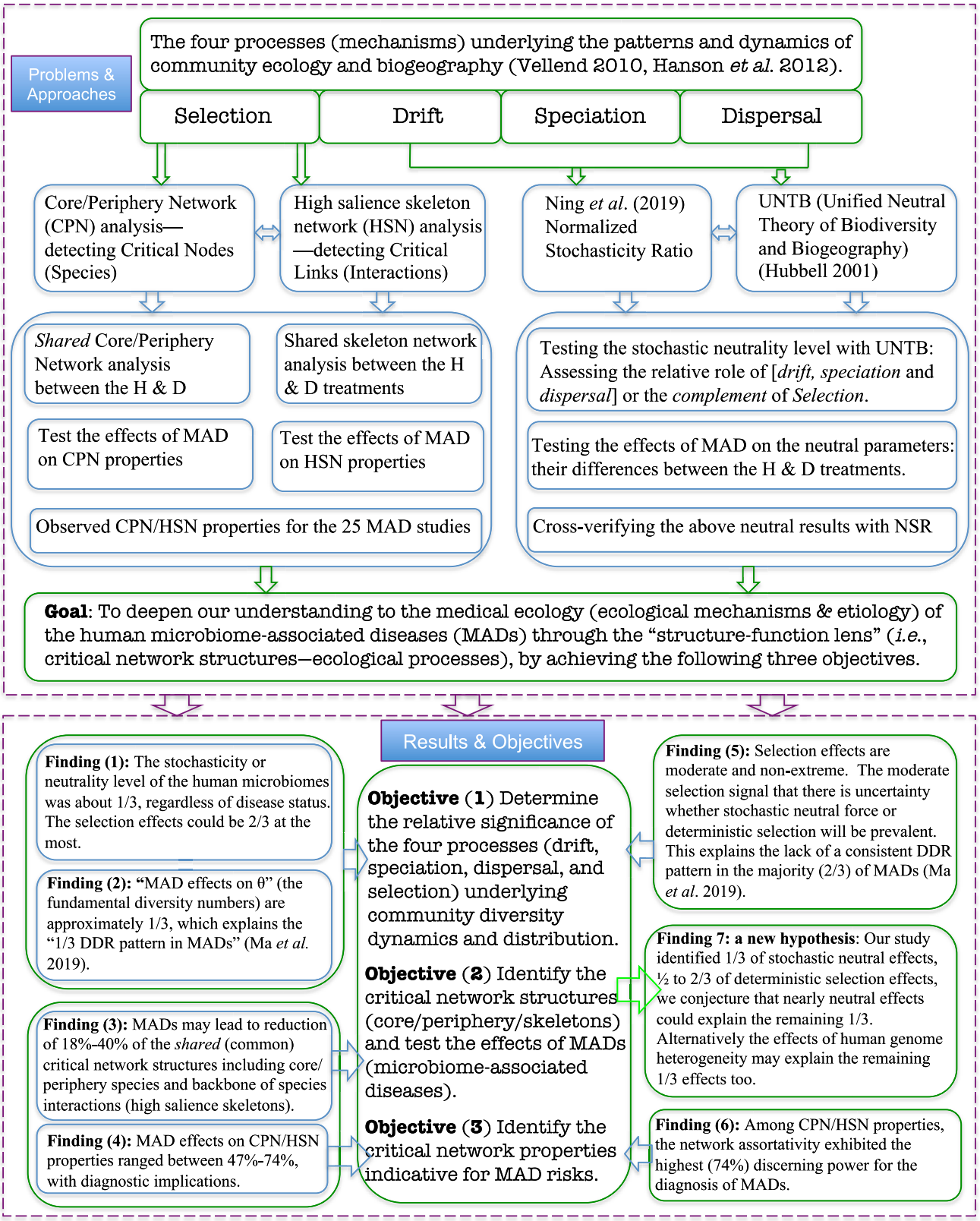
Problems & Approaches
The four processes (mechanisms) underlying the patterns and dynamics of community ecology and biogeography (Vellend 2010, Hanson *et al.* 2012).
Selection
Drift
Speciation
Dispersal
Core/Periphery Network (CPN) analysis—detecting Critical Nodes (Species)
High salience skeleton network (HSN) analysis—detecting Critical Links (Interactions)
Ning *et al.* (2019) Normalized Stochasticity Ratio
UNTB (Unified Neutral Theory of Biodiversity and Biogeography) (Hubbell 2001)
Shared Core/Periphery Network analysis between the H & D
Shared skeleton network analysis between the H & D treatments
Test the effects of MAD on CPN properties
Test the effects of MAD on HSN properties
Observed CPN/HSN properties for the 25 MAD studies
Testing the stochastic neutrality level with UNTB: Assessing the relative role of [*drift, speciation* and *dispersal*] or the *complement* of *Selection*.
Testing the effects of MAD on the neutral parameters: their differences between the H & D treatments.
Cross-verifying the above neutral results with NSR
Goal: To deepen our understanding to the medical ecology (ecological mechanisms & etiology) of the human microbiome-associated diseases (MADs) through the "structure-function lens" (*i.e.*, critical network structures–ecological processes), by achieving the following three objectives.
Results & Objectives
Finding (1): The stochasticity or neutrality level of the human microbiomes was about 1/3, regardless of disease status. The selection effects could be 2/3 at the most.
Finding (2): "MAD effects on θ" (the fundamental diversity numbers) are approximately 1/3, which explains the "1/3 DDR pattern in MADs" (Ma *et al.* 2019).
Finding (3): MADs may lead to reduction of 18%–40% of the *shared* (common) critical network structures including core/periphery species and backbone of species interactions (high salience skeletons).
Finding (4): MAD effects on CPN/HSN properties ranged between 47%–74%, with diagnostic implications.
Objective (1) Determine the relative significance of the four processes (drift, speciation, dispersal, and selection) underlying community diversity dynamics and distribution.
Objective (2) Identify the critical network structures (core/periphery/skeletons) and test the effects of MADs (microbiome-associated diseases).
Objective (3) Identify the critical network properties indicative for MAD risks.
Finding (5): Selection effects are moderate and non-extreme. The moderate selection signal that there is uncertainty whether stochastic neutral force or deterministic selection will be prevalent. This explains the lack of a consistent DDR pattern in the majority (2/3) of MADs (Ma *et al.* 2019).
Finding 7: a new hypothesis: Our study identified 1/3 of stochastic neutral effects, ½ to 2/3 of deterministic selection effects, we conjecture that nearly neutral effects could explain the remaining 1/3. Alternatively the effects of human genome heterogeneity may explain the remaining 1/3 effects too.
Finding (6): Among CPN/HSN properties, the network assortativity exhibited the highest (74%) discerning power for the diagnosis of MADs.

Figure 1. Diagram for the Study Design and Conclusions
Illustration of the goal, objectives, approaches, and results (main findings) from investigating the critical network structures and ecological processes (mechanisms) underlying the human microbiome-associated diseases.

ecology has been invoked to explain its etiology (Sobel, 1999; Ma et al., 2012; Li and Ma, 2019; Ma and Ellison, 2019). In other cases, microbiome may simply act as part of the host environment that influences the metabolism of hosts. Obesity may belong to such a case, where the role of gut microbiome, although extensively investigated in the last decade, is still hotly debated (Rastelli et al., 2018). In yet other cases, such as cancers and HIV, the involvement of microbiome may be indirect but can still be significant (Williams et al., 2016; Bandera et al., 2018). It is for these diverse scenarios we use the term "microbiome-associate disease" (MAD) in this study.

If the extensively investigated DDR in human MADs is inconsistent in the majority of cases (approximately two-thirds) (Ma et al., 2019; Ma, 2020a, 2020b), using diversity indexes as diagnostic indicators for MADs becomes minimally useful, not to mention its role in mechanistic/etiological studies of MADs. The present study therefore aims to search for possible alternatives, and here we focus on detecting the ecological/network "imprints" of MADs on the human microbiomes, which may help to reveal underlying ecological mechanisms of MADs and possibly act as diagnosis and risk prediction indicators for MADs (Figure 1). For example, the network assortativity is related to network resilience, and it was found that slightly disassocitative networks (negative assortativity but with small absolute value) are less resilient because network percolates less easily in such networks (Newman and Clauset, 2016). In this study, we test whether critical network structure and properties such as assortativity can be more indicative than standard diversity metrics such as Shannon entropy in detecting the effects of MADs. Besides identifying potentially more powerful network indicators for MAD effects, a second objective of the present study is to establish possible mechanistic links between the critical network structures (of microbiomes) and the *processes* that drive the microbiome dynamics, which is of obvious significance for deep understanding of the mechanisms and etiologies of MADs.

We resort to Hubbell (2001) unified neutral theory of biodiversity (UNTB) and network analyses (Figure 1). We dissect the influences of MADs on the community assembly and diversity maintenance by harnessing the power of UNTB, which covers the *three* processes (mechanisms) of Vellend-Hanson four-processes synthesis of community ecology and biogeography (Vellend, 2010, 2016; Hanson et al., 2012), including *drift*, *speciation* (*mutation*), and *dispersal* (Rosindell et al., 2011) (the other is *selection*), and by integrative analyses with core/periphery network (CPN) (Csermely et al., 2013; Ma and Ellison, 2019) and high-salience skeleton network (HSN) (Grady et al., 2012; Shekhtman et al., 2014; Ma and Ellison, 2019) modeling. The four-processes (mechanism) synthesis stated that, similar to the modern synthesis of population genetics, drift, speciation, dispersal, and selection constitute the underlying processes (mechanisms) that drive community dynamics and shape the microbial biogeography (the spatial and temporal distribution patterns of community diversity) (Vellend, 2010, 2016; Hanson et al., 2012). We argue that the CPN/HSN analyses possess the potential to assess and interpret the effects of *selection* in the four-processes synthesis as further elaborated below.

We realized that, since the UNTB optimizes the fit of the relative abundance to the predictions of the neutral model, it might over-estimate the true strength of neutral processes. Therefore, rather than examining the fit of the relative abundance data to the predictions (i.e., the passing rate of neutrality tests), we should focus on the estimated parameters of the neutral model (fundamental numbers of diversity and fundamental number of dispersal) and ask if they differ between healthy and diseased individuals. We also recognized that the four-processes synthesis is still largely conceptual in its current stage and refrained from inferring conclusions from it, particularly quantitative inferences. That said, in this article, we primarily depend on the analyses of critical network structures with the CPN and HSN (Csermely et al., 2013; Grady et al., 2012; Shekhtman et al., 2014; Ma and Ellison, 2019) and use neutral-theoretic approach and four-processes synthesis to cross-verify and supplement our findings (Figure 1).

According to Vellend (2010, 2016), *selection* refers to the deterministic fitness difference between individuals from different species, and it can also be treated as the deterministic interactions among species and between species and their environments. *Selection* represents asymmetric or unequal interactions; in other words, not all species or their interactions were "born" equal. From a conceptual perspective, we argue that *critical network structures* (core/periphery/skeleton/backbone) in the CPN/HSN can be considered as *outcome* of *selection* given their asymmetrical and heterogeneous nature. We argue that, conceptually, our integrated analyses (Figure 1) of the human MADs datasets with the UNTB (Hubbell, 2001), Ning et al.

(2019) ecological stochasticity framework, and CPN/HSN networks (Csermely et al., 2013; Grady et al., 2012; Shekhtman et al., 2014; Ma and Ellison, 2019) cover the full spectrum of all four processes (drift, dispersal, speciation, and selection) of Vellend-Hanson synthesis of community ecology and biogeography (Vellend, 2016; 2010; Hanson et al., 2012). Figure 1 summarizes the overall goal, objectives, datasets, approaches, as well as findings and conclusions of the present study.

RESULTS

A brief description on the metagenomic datasets of the 27 MAD studies, which are used to generate the results here, is provided in Table S1 of the Supplemental Information, which are the same datasets used in Ma et al. (2019). Among the 27 datasets, there were 3 and 2 datasets that are not suitable for the neutral-theoretic analysis and CPN/HSN analyses, respectively, and therefore were excluded from the analyses of this study. The 27 case studies cover most of the high-profile MADs, including obesity, IBD, diabetes, BV, periodontitis, and neurodegenerative diseases. The datasets were in the abundance of 16s-rRNA reads clustered at the species level (97% similarity level), equivalent with the species abundance tables in macrobial ecology.

This section is organized as eight subsections covering (see the bottom section of Figure 1): (1) the first three subsections on neutral theoretic analysis—testing the MAD effects on the microbiome neutrality and on the neutral model parameters (fundamental biodiversity/dispersal numbers) as well as estimating the normalized stochasticity ratio (NSR) to cross-verify the neutral-theoretic analyses; (2) two consequent subsections on the CPN—*shared* core/periphery network analysis between the healthy (H) and diseased (D) treatments and further testing the MAD effects on the key *CPN properties*; (3) followed by two subsections on the HSN (high-salience skeleton network)—*shared* skeleton network analysis and further testing the MAD effects on the key *HSN properties*; (4) finally, the actual (observed) key CPN/HSN network properties for the 25 MAD case studies. The consequent discussion section further summarizes our findings from the results presented in this section.

Neutral-Theoretic Analysis: Testing MAD Effects on the Microbiome Neutrality

Tables S2A–S2E exhibited the detailed results of the neutrality tests for the 24 case studies of MADs. For each case study, the neutrality test was performed for each community sample (from each individual subject) of the H (healthy) and D (diseased) treatments, separately. For each community sample, five data pre-processing schemes (*raw*—no preprocessing, *singleton*—removal of singleton, *minus–1*, *minus–2*, *minus–3*, i.e., removal of 1, 2, or 3 individuals across all OTUs, respectively) were implemented to obtain robust test results. What were displayed in Tables S2A–S2E included the key parameters of the classic neutral model, such as the fundamental biodiversity number (θ), migration probability (m), and p value for the neutrality test.

Table S3, summarized from Table S2, exhibited the neutrality passing rates for each of the 24 case studies. Table S4 exhibited the results of Fisher's exact probability test for determining the effects of MAD diseases on the passing rates of neutrality.

Figure 2, drawn based on Tables S2, S3, and S4, illustrated the passing rates for each case study. Note that Figure 2 was plotted with the *average* passing rates across the results obtained from five data pre-processing schemes. In Figure S1 (see Supplemental Information), the passing rate corresponding to each of the five data pre-processing schemes was plotted. Hence, Figure 2 here is a summary version of Figure S1.

From Figures 2 and S1, and Tables S2, S3, and S4, we summarize the following findings:

(1) Across the five data pre-processing schemes, the neutrality passing rates ranged from 26.2% to 78.3% with an average of 57% for the H treatments and ranged from 27.1 to 80.1 with an average of 60% for the D treatments. Given that the three schemes with minus 1, 2, or 3 across all OTUs achieved neutrality rates higher than the raw and singleton-removed schemes, obviously, the results from using raw datasets should be more robust if the objective is to obtain more conservative (reliable) estimation of the neutrality level. These results indicate that the human microbiome, regardless of the health/disease status, exhibited significant level of neutrality that cannot be ignored. In other words, at least, in close to one-third (H = 26.2% D = 27.1%) of the tested samples, the neutrality plays a predominant role in community assembly and diversity maintenance, and furthermore, the neutrality passing rates can be as high as 80% (78.3%–80.1%).

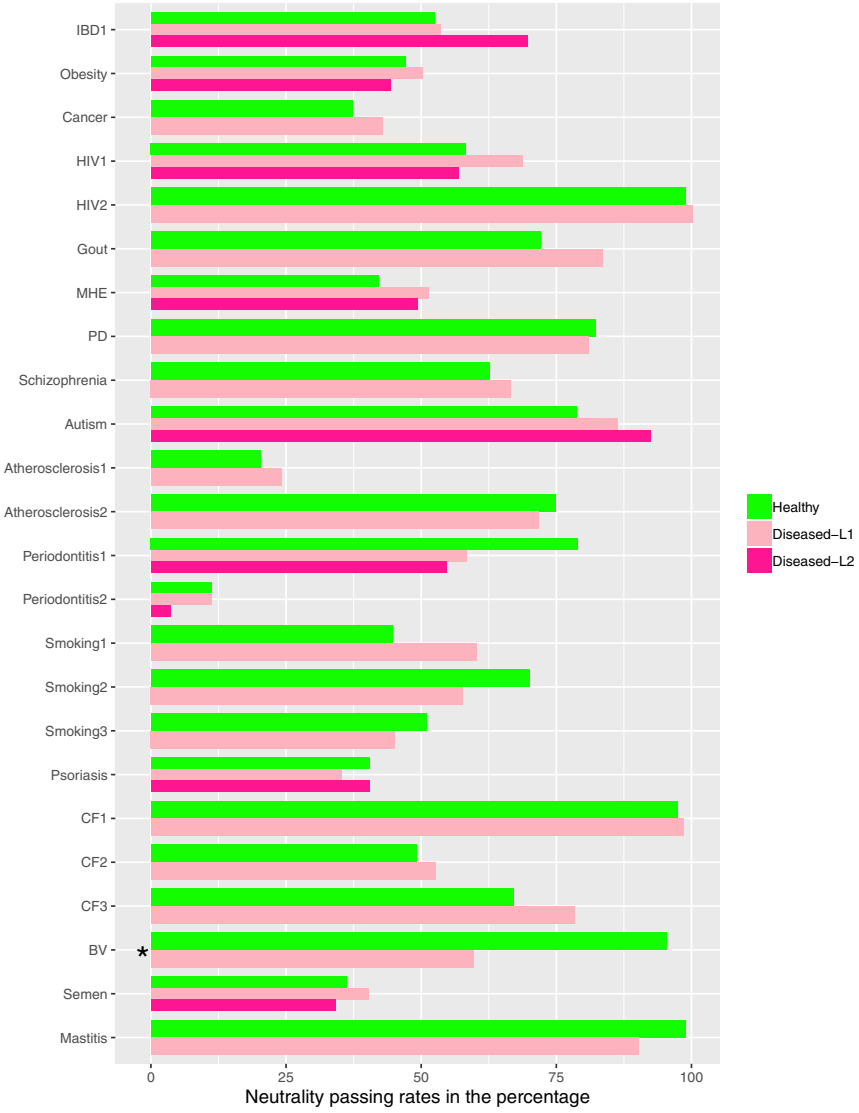

Figure 2. The Neutrality Passing Rates for Each of the 24 Case Studies

The neutrality passing rates for each of the 24 case studies: the cases with significant differences in the passing rates between the healthy and diseased treatments are marked with "*"; for each case study, the average percentage across five data-preprocessing schemes was computed and utilized to represent the neutrality of a case study.

(2) Fisher's exact probability test showed that, in absolute majority cases, diseases did not exert a significant effect on the neutrality passing rates (Table S4 and Figure 3). Specifically, in only 5 of 165 comparisons (3%), there were significant differences in the neutrality passing rates between the H and D microbiome samples.

Neutral-theoretic analysis: testing disease effects on the fundamental biodiversity number (θ) and fundamental dispersal numbers (m)

Table S5 listed the results of the significance tests for θ (the fundamental biodiversity numbers), which is a measure of *speciation*, and for m (the migration probability or fundamental dispersal numbers), a measure for *dispersal limitation*, between the H and D samples. The Wilcoxon test was performed to determine whether or not MAD could have significant influence on the parameters (θ and m). Figure 3 displayed the average values of m and θ (across five data pre-processing schemes) for each case study, and it also marked the cases with significant differences between the H & D treatments. Note that Figure 3 (a summary

Figure 3. The Key Parameters from Neutral-theoretic Modeling

The fundamental diversity number (θ) and immigration probability (m) for each of the 24 case studies, and the cases with significant differences in the parameters between the healthy and diseased treatments are marked with "*"; for each case study, the average parameters across five data-preprocessing schemes are used to plot the figure.

version of Figures S2 and S3) was plotted with the *average* parameters across five data pre-processing schemes. In Figures S2 and S3, the parameters for each of the five data pre-processing scheme were plotted.

The findings from the significance tests (Table S5 and Figures 3, S2, and S3) seem rather consistent across five different data-preprocessing schemes. In approximately one-third (30%–33%) of the comparisons, the fundamental biodiversity numbers (θ) were significantly different between the H and D treatments. In only approximately 15% of the comparisons (9.1%–21.2%), the migration probabilities (m) were significantly different between the H and D treatments. These findings suggest that diseases have significant influences on the *speciation* in approximately one-third of the comparisons, whereas significant influences exist in only 15% of the comparisons in term of the *dispersal limitation*.

Cross-Verification of Neutral Theoretic-Analyses with Normalized Stochasticity Ratio

As explained previously, the optimized fitting of UNTB is likely to lead to overestimation of the stochastic neutral levels. We apply Ning et al. (2019) framework for estimating community stochasticity level, specifically NSR (Table S6 and Figure 4), for cross-verifying the previous UNTB results. Table S6 included the mean NSRs for the intra-H (intra-healthy), intra-D (intra-diseased), and inter-HD (healthy versus diseased) treatments, respectively, as well as the p values from the Wilcoxon tests of the differences in the NSR among the three treatments. Figure 4 illustrated the contents listed in Table S6, i.e., the NSRs for each treatment in the 27 MAD cases, and the treatments with statistically significant differences were marked with star (*). From Table S6 and Figure 4, we summarize the following four findings, which can be used to verify/calibrate the previous UNTB results.

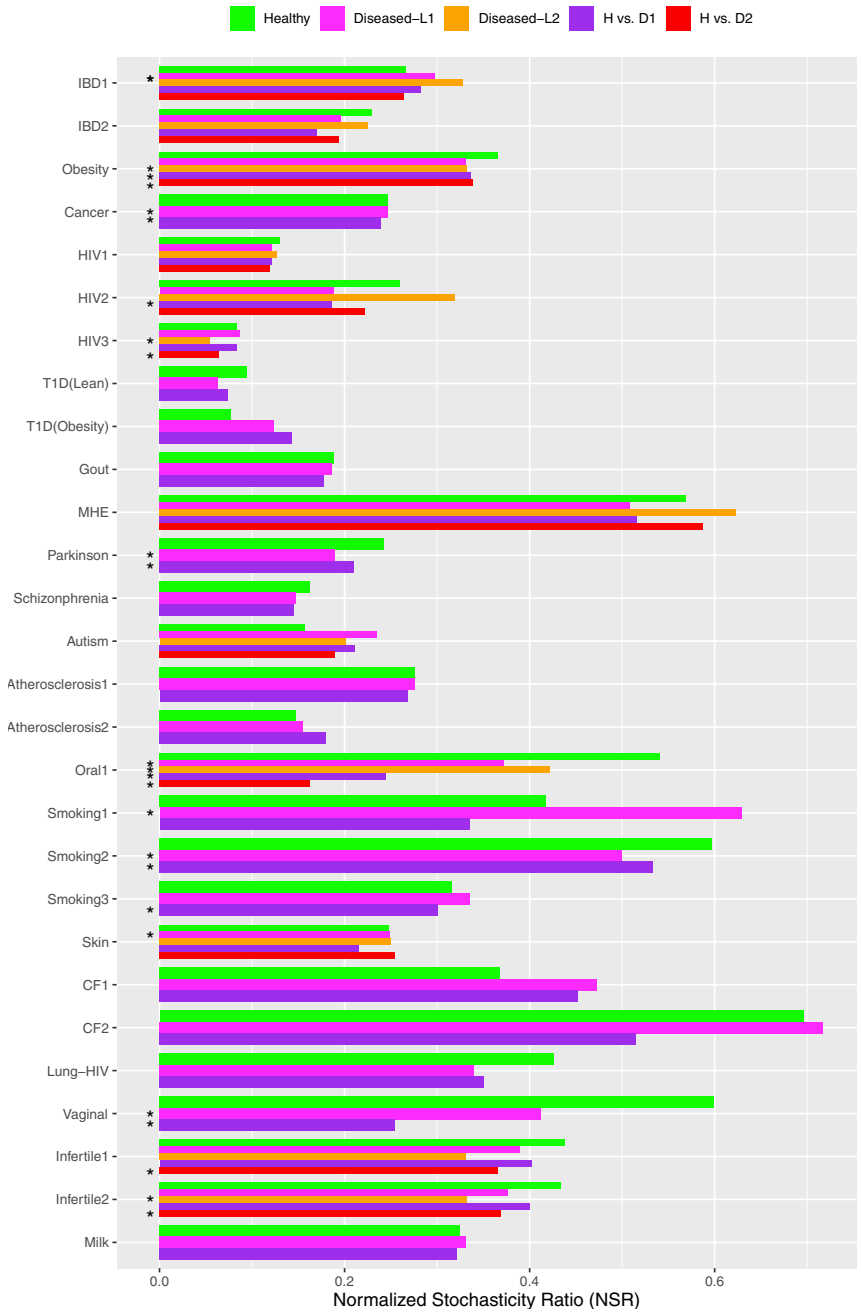

Figure 4. The NSR (Normalized Stochasticity Ratio)

The NSR (normalized stochasticity ratio) for each of the 27 case studies: the treatments with significant differences in NSR were marked with star (*).

(1) The average NSR for intra-H, intra-D, and inter-HD is 0.342, 0.334, and 0.287, respectively. The slightly decreased NSR in this order suggests that diseases might cause the decline of stochasticity. Among the three NSRs, the difference between intra-H (0.342) and inter-HD (0.287) should be a more objective indicator for disease effects, which is about 16% roughly in terms of the "*face*" values of NSRs. Further rigorous *statistical tests* with Wilcoxon tests indicate that, in 30% of the MAD cases (12 of 40 possible comparisons between H and D) comparing the intra-H and intra-D treatments exhibited significant differences in their NSRs. The percentage is slightly lower (27.5% or 11 of 40) after FDR (false discovery rate) control is applied.

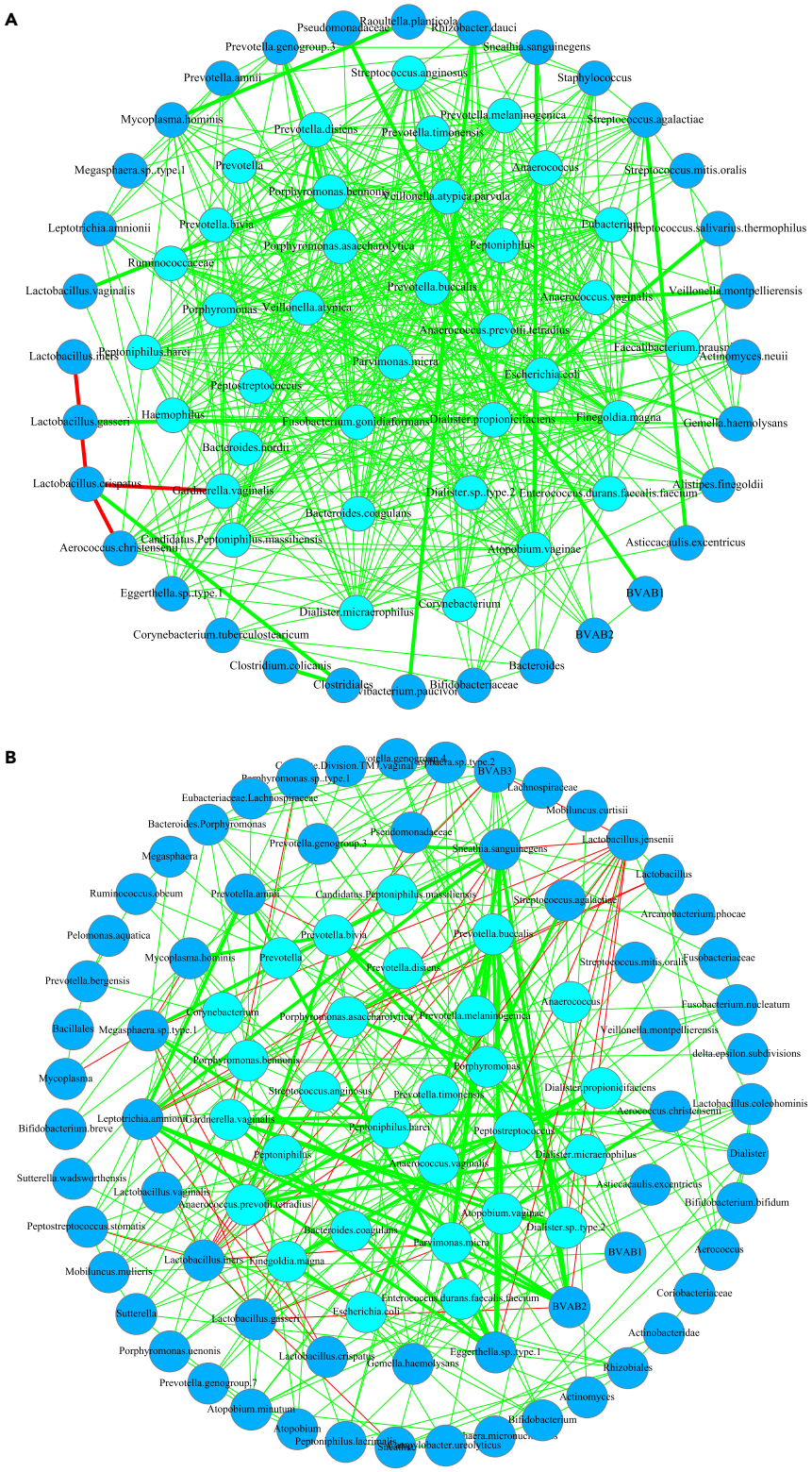

Figure 5. Network Graphs Illustrated with BV (Bacterial Vaginosis) Study

The core/periphery/skeleton network for the healthy (A) and BV (B) treatment, respectively, and the legends used include: the core nodes, circle in cyan; the periphery nodes, circle in dodger blue; regular positive links, regular lines in green;

Figure 5. *Continued*
high-salience positive skeleton (links), thick lines in green; regular negative links, regular lines in red; high-salience negative skeleton (links), thick lines in red.

(2) Since the NSR was normalized to the range between 0 and 1 and is a ratio (hence dimensionless), the range of 0.297–0.334 also indicates the general stochasticity level in the human microbiome, regardless of diseases status, is rather tight, i.e., around *one-third*. Compared with the findings from previous UNTB modeling, i.e., the range between 26.2% and 78.3% for the H treatments, and the range between 27.1 and 80.1 for the D treatments, the NSR range is rather close to the *floor* limits of the neutral modeling. If we accept the conjecture that UNTB tends to overestimate the stochastic neutral forces, it should be safe to conclude that the neutrality-passing rate or stochasticity level in the human microbiome should be about one-third, and the upper range (up to 80%) may indeed be unduly overestimated.

(3) As to the MAD effects, the previous tests with fundamental dispersal numbers (migration probability) and fundamental biodiversity numbers (speciation rate) indicated 15% (dispersal) to 33% (biodiversity) of the comparisons, and the NSR here revealed a similar effect size (30%–32.5%) based on Wilcoxon tests. Therefore, we conclude that the MAD effects on the neutral processes are in the range between 15% and 33% (=1/3) approximately, depending on whether dispersal (migration) or biodiversity is considered, with the former receiving a lower impact than the latter.

Core/Periphery Network Analysis: Shared Core/periphery Analysis

Shared core/periphery nodes analyses (SCA/SPA) aim to detect the effects of MADs on the numbers of shared core/periphery species (nodes) between the H and D treatments because the decline of shared nodes may signal the effects of MADs. Table S7 listed the results from shared core species (nodes) (the left side) and periphery species (nodes) (the right side) analyses between the H and D treatments. The randomization tests were performed based on 1,000 sets of CPNs built with FDR (false discovery rate) control and p value = 0.001, which ensures only significant correlations based on Spearman's correlation coefficient are admitted into the species correlation networks (SCN). From the SCNs (species correlation networks), the corresponding CPNs were constructed based on the algorithms previously introduced. Figure 5 illustrates the graphs of CPN and HSN (high-salience skeleton network) with BV case study as examples.

In Table S7, both the observed (actual) shared nodes and permutated (simulated) nodes were listed for the core and periphery, respectively. The p value from comparing the observed- and permutated-shared species (nodes) is used to determine whether or not the shared species (core or periphery) between the H and D treatments decreased more than by chance. When the p value <0.05, the shared core or periphery species were reduced more than the decrease by chance; in other words, disease caused the reduction of shared nodes (core or periphery species). Otherwise, the reduction of shared nodes was not caused by disease, instead by chance.

The bottom section of Table S7 exhibited the percentages (%) of MAD cases with decreased shared core (24%) or periphery (18%) species, respectively. Figure 6 illustrated the same information listed in Table S7. The cases with decreased shared species (core or periphery) were marked with star (*).

Core/Periphery Network Analysis: Testing the Differences in CPN Properties

Table S8 listed the p values from testing the differences in the CPN properties (parameters) between the H and D treatments. The CPN properties tested include core strength (ρ), the fraction of core nodes, the four components of core density matrix, and the network nestedness. The randomization tests were performed again based on the same 1,000 sets of permutated networks used in the shared core/periphery analysis above, but the algorithm used was slightly different (see the Supplemental Information for the related algorithms).

Table S8 shows that the disease effects on the CPN properties ranged from 45% to 64%; in all but two properties [C/(C + P) and B12/B21], the percentage with significant differences exceeded 50%. The parameter with the highest percentage in the difference between the H and D is B22, which represents the interactions among the periphery nodes. This should be expected since periphery nodes are weakly connected and more likely influenced by perturbations such as diseases.

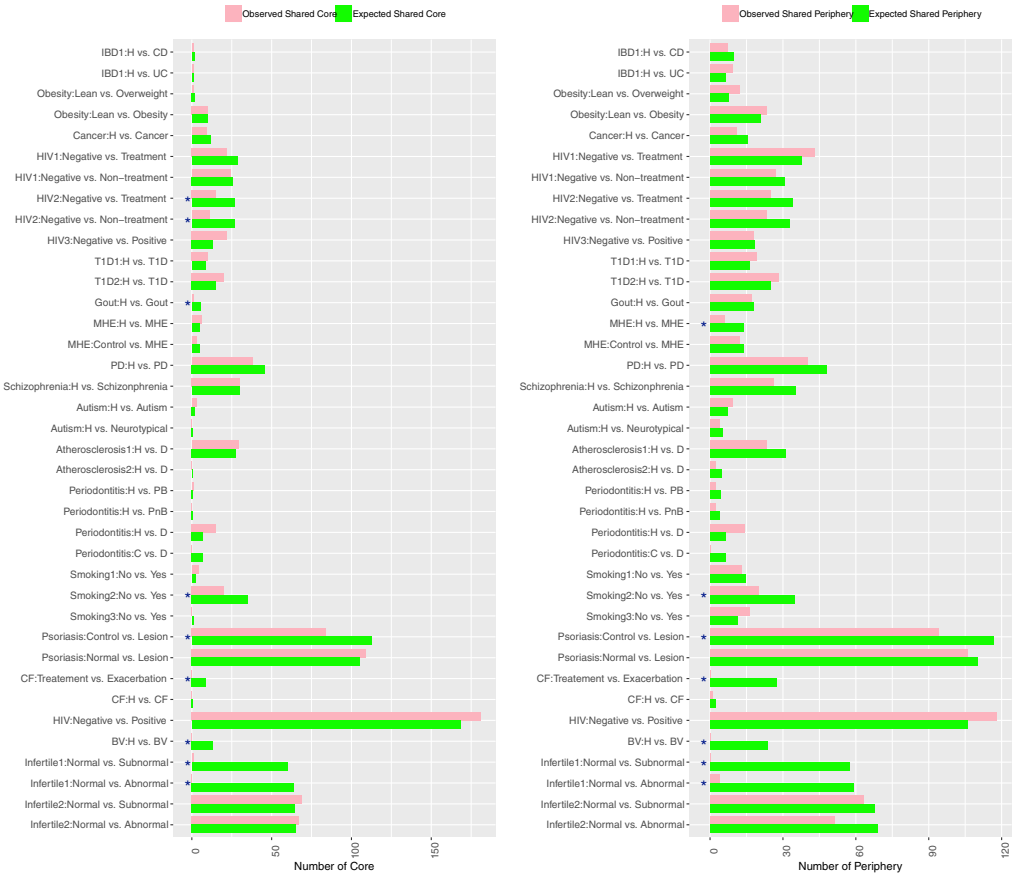

Figure 6. Share Core/Periphery Node Analysis

The numbers of *shared* core (the left graph) or periphery (the right graph) species (nodes) between the healthy (*H*) and diseased (*D*) treatments: the permutation test was performed with 1,000 pairs (pair = H and D) of permutated networks ("*": represents the cases with significant difference between the *H* and *D*). The figure is plotted based on Table S6.

High-Salience Skeleton Network Analysis: Shared Skeleton Analysis

Table S9 listed the results from shared skeleton analysis between the H and D treatments. The randomization test was performed based on 1,000 sets of permutated HSNs built with FDR control and p value = 0.001. In Table S9, both the observed (actual) shared skeletons and permutated (simulated) skeletons were listed. The p value from comparing the observed- and permutated-shared skeletons is used to determine whether or not the shared skeletons between the H and D treatments decreased more than the decrease by chance. When p value <0.05, the shared skeleton was reduced more than the decline by chance; in other words, disease caused statistically significant reduction of shared skeletons. Otherwise, the reduction of shared skeletons was not caused by disease, instead by chance.

The bottom section of Table S9 exhibited the percentages of MAD cases with decreased shared skeletons (40%). Figure 7 illustrated the same information listed in Table S9. The cases with declined shared skeletons were marked with star (*). The percentage with significant decline in shared skeleton is higher than the percentage of shared core (24%) and shared periphery (18%) in the previous subsection. This difference suggests that diseases have more far reaching influences on the interactions (skeletons) than on the species per se (nodes).

High-Salience Skeleton Network Analysis: Testing the Differences in HSN Properties

Table S10 listed the p values from testing the differences in the HSN properties between the H and D treatments. The HSN properties tested include links% (the percentage of high salience skeletons), the max, mean, skewness, and kurtosis of the salience values, as well as *assortativity* (a measure of network resilience). The randomization tests were performed based on the same 1,000 sets of permutated networks

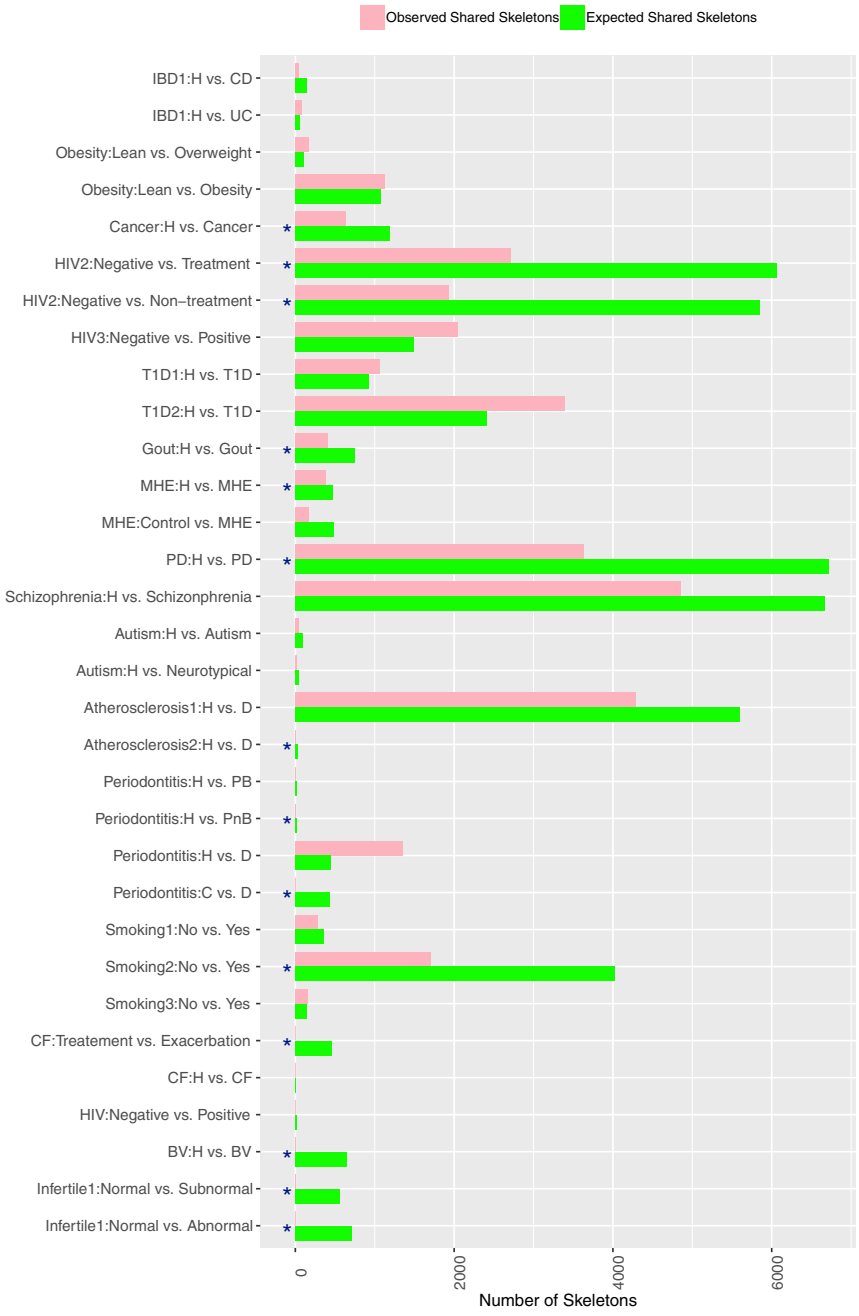

Figure 7. Share High-Salience Skeleton Analysis

The numbers of *shared* high-salience skeletons (*HSS*>0) between the healthy (*H*) and diseased (*D*) treatments: the permutation test was performed with 1,000 pairs (pair = *H* and *D*) of permutated networks ("*": represents the treatments with significant difference between *H* and *D*). The figure is plotted based on Table S8.

used for the previous shared skeleton analysis, but the algorithm is slightly different from that used in the shared skeleton analysis and is the same as that used for testing the CPN properties previously (see the Supplemental Information).

Table S10 shows that the effects of diseases on the HSN properties ranged from 47% to 74%, and in all but one property (skewness), the percentages with significant differences exceeded 50%. The highest percentage in the difference between the H and D occurred in assortativity (r_{HSS} = 74%), which represents for the

assortativity of HSN and measures the resilience of the network. This suggests that, in approximately three-fourth (74%) studied cases, diseases significantly impact the network resilience. This finding cross-validated the previous finding from shared skeleton analysis, i.e., diseases exert more far-reaching effects on species interactions (skeletons) than on the species per se (nodes).

The Key Properties of Critical Network Structures (Core/Periphery/Skeletons)

The core/periphery nodes and high-salience skeletons represent for the critical structures of the species interactions in the community (network), from either node or link perspective. In the previous sub-sections, we focused on statistical (permutation) tests for the potential differences between the H and D treatments in terms of either *shared* critical network *structures* (core/periphery/skeleton) or their *network properties*. In this sub-section, we briefly introduce the key properties of those critical network structures *per se*, for example, the list of shared or unique core species in the H or D treatment in the SI.

Table S11 listed the key network properties of the CPN for each of the 25 MAD case studies, including the core strength (ρ), fraction of core nodes, density matrix of core/periphery structure, and network nestedness. For example, the average core strength (ρ) for the healthy and diseased treatments is 0.175 versus 0.216, with standard error of 0.026 versus 0.033. Theoretically, ρ ranges from 0 to 1 and represents for the relative strength of core structure. The range indicates that the strength of human microbiome networks is relatively loose. As shown in Table S8, ρ is significantly different between the H and D treatments in approximately 60% of the MAD cases. Similarly, Table S12 listed the key network properties of the HSN for each of the 25 MAD cases. As exhibited in Table S10 previously, almost all HSN properties showed significant difference between the H and D individuals in more than half of the 26 MAD cases, and in particular, the assortativity of high-salience skeletons differed in 74% of the cases.

Tables S13–S15 further listed the actually *observed* number of shared core nodes, *observed* number of shared periphery nodes, and *observed* number of shared skeletons, respectively, shared between the H and D treatments in each of the 25 MAD datasets. Those three tables exhibited the actually *observed* levels of similarity (shared core/periphery/skeletons) between the H and D treatments and deserve further investigations aimed to understand specific disease mechanisms/etiologies.

CONCLUSIONS AND DISCUSSION

Ecologists often seek to understand the relationships between the *structure* and *function (process)* of ecological systems to deepen their understanding to ecological mechanisms. Nonetheless, this relationship is rarely straightforward, and what is being seen (i.e., community or network structure) must be filtered and analyzed carefully before committing a belief on what is going on in the system (e.g., *community stability*). This is because structure is usually only an imperfect and often ambiguous manifestation of the process (Ma, 2015). In the case of this study, we aimed to detect the relationships between critical community (network) structures and disease effects (states) beyond the findings revealed in our previous DDR, in which we found that in only approximately one-third of the MAD cases disease states were related to diversity measures, but in the majority of cases (approximately two-thirds) there was not a consistent DDR pattern (Ma et al., 2019). In the present study, we focus on detecting the ecological/network "imprints" of MADs on the human microbiomes, which may help to reveal underlying ecological mechanisms of MADs and possibly act as diagnosis and risk prediction indicators for MADs. Such explorations are important because revealing the relationships (imprints) is critical not only for understanding the disease mechanisms/etiologies but also for developing diagnosis and/or risk prediction techniques. Methodologically, we introduced three approaches to looking into the structure-mechanism paradigms in the medical ecology of the human MADs, including Hubbell (2001) UNTB, Ning et al. (2019) framework for stochasticity assessment, and CPN/HSN networks (Csermely et al., 2013; Grady et al., 2012; Shekhtman et al., 2014; Ma and Ellison, 2019). Here, we further summarize the following seven findings from the previous sections and discuss their implications. It should be noted that the findings are supported by the analyses introduced in previous sections, but the implications may include postulations or even speculations.

Finding (1)

The *stochasticity* or *neutrality* level, in the human microbiomes of the MAD case studies we analyzed, was approximately one-third, which is revealed by Hubbell (2001) UNTB testing, cross-verified by Ning et al.

(2019) stochasticity analysis framework. The disease status of MADs did not significantly influence the stochasticity/neutrality level. The implications of this finding are as follows:

Since the neutrality level is a measure of stochastic drift, speciation, and dispersal (i.e., three of the four processes of Vellend-Hanson synthesis) (Rosindell et al., 2011; Vellend, 2010; Hanson et al., 2012), it indicates the extent or level (i.e., one-third) that the microbial community is driven by the stochastic neutral forces. We might further postulate that the deterministic *selection* (i.e., the other process in the four process of Vellend-Hanson synthesis) (Vellend, 2010, 2016; Hanson et al., 2012) could be $(1 - 1/3) = 2/3$ at the most. However, this postulation is contingent on the *additivity* of the four processes of the synthesis, which is still an open question.

Finding (2)

In approximately one-third of the cases analyzed, MADs had significant effects on the fundamental biodiversity numbers (θ), whereas the MAD effects on the fundamental dispersal numbers (m) were approximately 15%. Therefore, although MADs did not significantly influence the mode (nature of mechanism) of microbiome assembly and diversity maintenance—whether the mechanism is stochastic or deterministic, as indicated by Finding (1) above—MADs may indeed have certain level of effects on the microbiome diversity and the upper bound (ceiling) seems to be one-third as indicated by the disease effects on θ.

This "one-third MAD effects on θ (the fundamental biodiversity number)" offers a mechanistic interpretation for the "one-third DDR pattern" (i.e., in only approximately one-third of the MAD cases, diversity is related to disease status) from our previous DDR analysis (Ma et al., 2019).

Finding (3)

The critical network structures detected with CPN/HSN analyses revealed that MADs can lead to significant reductions of *shared* (common) core/periphery/skeleton structures, approximately 24%, 18%, and 40% respectively. That is, there should be disease-specific core/periphery (species) and skeletons (species interactions). First principles suggest that disease may lead to divergence between the H (healthy) and D (diseased) individuals, consequently the reduction of *shared* (common) critical structures. Therefore, the reduction of shared critical structures should be expected.

Finding (4)

Besides influencing the *shared* critical network structures (which ranged between 18% and 40%), as stated above, the MAD effects on the CPN properties ranged between 45% and 64% depending on specific CPN properties and the MAD effects on the HSN properties ranged between 47% and 74%. The difference between the "*shared* critical network *structures*" and "network (CPN/HSN) *properties*" lies in that the former is *holistic* and *structural* and the latter is a collection of network properties that may reflect either *global* or *local* network characteristics.

Summarizing Findings (3) and (4), we conclude that, for diagnostic and/or risk assessment purposes, the properties (particularly *network assortativity*) of critical network structures can be more promising than the numbers of network structures per se, and also more promising than the neutral theory parameters, given that the MAD effects on most of the network properties exceeded half. The most promising network property reflecting the microbiome resilience against MADs seems to be *network assortativity*, which reached 74% of differences between the H and D treatments, which is discussed further below in Finding (6).

Finding (5)

Selection is the difference in the deterministic fitness between individuals from different species, and it can also be treated as the deterministic interactions among species and between species and their environments (Vellend, 2010, 2016). The former definition emphasizes the outcome of selection at the individual level, and the latter definition emphasizes the process selection occurs at the species level. According to these definitions, what CPN/HSN analyses reveal, including the asymmetrical and heterogeneous network structures (i.e., core/periphery/skeleton), can be considered as the outcome of *selection*.

Therefore, the selection effects should range from 18% to 74% but range between 40% and 60% in terms of the most metrics, depending on the kinds of critical network structures or their properties. We consider that the selection effects ranged between 40% and 60% in terms of the most metrics are *moderate* and *non-extreme*. According to Vellend (2010, 2016), selection may vary across space or time, with potentially important consequences for community dynamics. Furthermore, when selection is relatively strong and the community size is large, any effects of drift may be canceled by selection. However, when selection is relatively weak and the community size is small, the opposite can occur, i.e., drift can override selection effects. Between the two previously conceived extremes, i.e., being moderate or non-extreme, selection could make some community states more likely than others, but it does not guarantee any particular state (outcome) (Nowak, 2006; Vellend, 2010, 2016). As we argued previously, the selection effects in human microbiomes should be *non-extreme* or *moderate*. We postulate that, according to Nowak (2006) and Vellend (2010, 2016), it is expected that, in the majority of cases, selection forces may not override the neutral forces nor be overridden by neutral forces. There is no guarantee that the community will be in any particular state (outcome). This *uncertainty* (*unpredictability*) may explain the lack of a consistent DDR pattern in the majority (approximately two-thirds) of MAD cases analyzed by Ma et al. (2019).

Finding (6)

The network assortativity is related to network resilience. It was found that slightly disassocitative networks (negative assortativity but with small absolute value) are less resilient (Newman and Clauset, 2016). Table S12 showed that the average assortativity of H and D is −0.041 and −0.022, respectively. Hence, the D treatments should be less resilient than the H treatments, which were the case in 74% of the 25 MAD cases, as revealed by the randomization tests exhibited in Table S10. In fact, the assortativity of HSN is the property that exhibited the highest divergence (74%) between the H and D treatments we discovered in this study. This finding may not be incidental given that assortativity can be considered as a measure of network resilience and loss of resilience or dysbiosis is well recognized as a hallmark of MADs.

Finding (7)

The last finding here is indirectly inferred from the previous six findings and is more speculative. Throughout the study, it appears that we could not break the *ceiling* limits of "one-third" in the case of neutral theory modeling or "half to two-thirds" in the case of network analysis regarding disease effects (also see Ma et al., 2019; Ma, 2020a, 2020b). The reality that we could not break the limits should not be surprising. Besides the possible imperfectness of the "structure-process (mechanism)" strategy our approaches followed, we expect a major source for the *unexplained* gap in disease effects or lack of MAD effects should be the *intrinsic* stability (resilience) of human microbiome against disturbances including diseases. The intrinsic resilience should primarily be due to *host genomes*, which should be rather stable at ecological timescale, the scale MADs occur. Therefore, we conjecture that the genome effects on the MADs should be approximately one-third or even more. Alternatively, we conjecture that the remaining unexplained MAD effects could be due to *nearly neutral forces* (Ohta, 2008; He et al., 2012). Compared with animal and plants, bacterial species seem to resemble each other closely in their demographic parameters but may not be the exactly same as the neutral theory assumes; consequently, *nearly neutral effects* could be significant. Finally, Figure 1 further summarized the above-discussed seven findings.

Limitations of the Study

The present study was aimed to investigate the critical network structures and medical ecology mechanisms underlying the human MADs, and it was a direct extension to our previous works in this field, based on the same MAD datasets but was approached with different objectives, analytic methods, and ecological theories (Ma et al., 2019; Ma, 2020a; 2020b). The most important limitations of our works have been discussed in Finding (7) in the previous section, which summarized the issues and proposed a conjectural hypothesis for further investigations. An additional limitation is that the scope of MAD datasets was limited to the marker gene (16s-rRNA) sequencing reads obtained from amplicon sequencing technology, and the metagenome datasets from the whole-genome sequencing (shotgun sequencing) were not implicated in this serious of studies (Ma et al., 2019; Ma, 2020a; 2020b). Both types of metagenomics studies (datasets) have not only different data structures (matrices of OTU abundances versus matrices of metagenomic gene abundances) but also very different bioinformatics and subsequent analytic approaches. In particular, there have been relatively few ecological approaches to the metagenomic gene abundance (GA) datasets. We argue that the lag in the applications of ecological theories for GA studies is not because of the applicability or importance of ecological theories; instead it is because of the enormous difficulties in analyzing the big data of metagenomic genes (the number

of which is orders of magnitude larger than the number of OTUs in the case of human microbiomes), which made subsequent ecological analyses rather difficult. To deal with the difficulty, we have been developing the applications of major ecological theories for the metagenomic GA datasets in another series of studies (Ma and Li, 2018; Ma, 2020c; Ma and Ellison, 2020). We argue that the medical ecology of human microbiomes, which can be considered as a cross-disciplinary field of microbiology, medicine, ecology, and bioinformatics (Ma, 2017; Ma et al., 2016), is complete only if both microbial OTUs and metagenomic genes are included. Therefore, future studies to complement the present study based on metagenomic GA datasets are certainly worthy of further explorations.

Resource Availability

Lead Contact

Sam Ma: ma@vandals.uidaho.edu.

Material Availability

N/A.

Data and Code Availability

All datasets analyzed in this study are available in public domain, and see Table S1 for the access information. All software codes are available in public domain as cited in the paper.

METHODS

All methods can be found in the accompanying Transparent Methods supplemental file.

SUPPLEMENTAL INFORMATION

Supplemental Information can be found online at https://doi.org/10.1016/j.isci.2020.101195.

ACKNOWLEDGMENTS

I appreciate Prof. Nicholas Gotelli, University of Vermont, USA, for his review, suggestions, and comments, for an early version of this manuscript, which played an important role in improving this manuscript. I am indebted to the anonymous reviewers and Dr. Simona Fiorani, the iScience Lead Editor, for their insightful comments and suggestions, which helped to improve my manuscript significantly. I thank Mr. L.W. Li and Miss Wendy Li of the Chinese Academy of Sciences for their computational support to this study. This study received funding from the following sources: A National Natural Science Foundation of China (NSFC) Grant (No. 31970116) on Medical Ecology of Human Microbiome; The Cloud-Ridge Industry Technology Leader Award; An International Cooperation Grant (YNST) on Genomics & Metagenomics Big Data. The funders played no roles in interpreting the results.

AUTHOR CONTRIBUTIONS

Z.S.M. designed and performed the study and wrote the manuscript.

DECLARATION OF INTERESTS

The author declares no competing interests.

Received: August 30, 2019
Revised: March 28, 2020
Accepted: May 21, 2020
Published: June 26, 2020

REFERENCES

Bandera, A., Benedetto, D.I., Bozzi, G., and Gori, A. (2018). Altered gut microbiome composition in HIV infection: causes, effects and potential intervention. Curr. Opin. HIV AIDS *13*, 73–80.

Castaño-Rodríguez, N., Underwood, A.P., Merif, J., Riordan, S.M., Rawlinson, W.D., Mitchell, H., Mitchell, H.M., and Kaakoush, N.O. (2018). Gut microbiome analysis identifies potential etiological factors in acute gastroenteritis. Infect. Immun. *86*, e00060–18.

Csermely, P., London, A., Wu, L.Y., and Uzzi, B. (2013). Structure and dynamics of core/periphery networks. J. Complex Netw. *1*, 93–123.

Duvallet, C., Gibbons, S.M., Gurry, T., Irizarry, R.A., and Alm, E.J. (2017). Meta-analysis of gut microbiome studies identifies disease-specific and shared responses. Nat. Commun. *8*, 1784.

Grady, D., Thiemann, C., and Brockmann, D. (2012). Robust classification of salient links in

complex networks. Nat. Commun. https://doi.org/10.1038/ncomms1847.

Hanson, C.A., Fuhrman, J.A., Horner-Devine, M.C., and Martiny, J.B.H. (2012). Beyond biogeographic patterns: processes shaping the microbial landscape. Nat. Rev. Microbiol. *10*, 497–506.

He, F.L., Zhang, D.Y., and Lin, K. (2012). Coexistence of nearly neutral species. J. Plant Ecol. *5*, 72–81.

HMP Consortium (2012). Structure, function and diversity of the healthy human microbiome. Nature *486*, 207–214, https://doi.org/10.1038/nature11234.

Hubbell, S.P. (2001). The Unified Neutral Theory of Biodiversity and Biogeography (Princeton University Press).

Integrative HMP (iHMP) Research Network Consortium (2019). The integrative human microbiome project. Nature *569*, 641–648. https://www.nature.com/articles/s41586-019-1238-8.

Johnson, P.T.J., Preston, D.L., Hoverman, J.T., and Richgels, K.L.D. (2013). Biodiversity decreases disease through predictable changes in host community competence. Nature *494*, 230–234.

Johnson, P.T.J., Ostfeld, R.S., and Keesing, F. (2015). Frontiers in research on biodiversity and disease. Ecol. Lett. *18*, 1119–1133, https://doi.org/10.1371/journal.pone.0041606.

Li, W., and Ma, Z.S. (2019). Diversity scaling of human vaginal microbial communities. Zoolog. Res. *40*, 587–594.

Lotter, H., and Altfeld, M. (2019). Sex differences in immunity. Semin. Immunopathol. *41*, 133–135.

Ma, Z.S. (2015). Power law analysis of the human microbiome. Mol. Ecol. *24*, 5425–5428.

Ma, Z.S. (2017). Bioinformatics: Computing and Software (Science Press).

Ma, Z.S. (2018). The P/N (Positive-to-Negative links) ratio in complex networks—a promising in silico biomarker for detecting changes occurring in the human microbiome. Microb. Ecol. *75*, 1063–1073.

Ma, Z.S. (2020a). Testing the Anna Karenina principle in human microbiome-associated diseases. iScience. https://doi.org/10.1016/j.isci.2020.101007.

Ma, Z.S. (2020b). Heterogeneity-disease relationship in the human microbiome associated diseases. FEMS Microbiol. Ecol. https://doi.org/10.1093/femsec/fiaa093.

Ma, Z.S. (2020c). Assessing and interpreting the metagenome heterogeneity with power law. Front. Microbiol. https://doi.org/10.3389/fmicb.2020.00648.

Ma, Z.S., and Ellison, A.M. (2019). Dominance network analysis provides a new framework for studying the diversity-stability relationship. Ecol. Monogr. *89*, e01358. https://esajournals.onlinelibrary.wiley.com/doi/full/10.1002/ecm.1358.

Ma, Z.S., and Ellison, A.M. (2020). Towards a unifying diversity-area relationship (DAR) of species- and gene-diversity. bioRxiv. https://doi.org/10.1101/2020.05.16.099861.

Ma, Z.S., and Li, L.W. (2018). Measuring metagenome diversity and similarity with Hill numbers. Mol. Ecol. Resour. *18*, 1339–1355.

Ma, Z.S., and Ye, D. (2017). Trios—promising *in silico* biomarkers for differentiating the effect of disease on the human microbiome network. Sci. Rep. *7*, 13259.

Ma, B., Forney, L.J., and Ravel, J. (2012). The vaginal microbiome: rethinking health and disease. Annu. Rev. Microbiol. *66*, 371–389.

Ma, Z.S., Guan, Q., Ye, C., Zhang, C., Foster, J.A., and Forney, L.J. (2015). Network analysis suggests a potentially 'evil' alliance of opportunistic pathogens inhibited by a cooperative network in human milk bacterial communities. Sci. Rep. *5*.

Ma, Z.S., Li, L., Li, W., Li, J., and Chen, H. (2016a). Integrated network-diversity analyses suggest suppressive effect of Hodgkin's lymphoma and slightly relieving effect of chemotherapy on human milk microbiome. Sci. Rep. *6*, 28048.

Ma, Z.S., Li, L.W., and Gotelli, N.J. (2019). Diversity-disease relationships and shared species analyses for human microbiome-associated diseases. ISME J. https://doi.org/10.1038/s41396-019-0395-y.

Ma, Z.S., Zhang, C., Zhang, Q., Li, J., Li, W., Qi, L., and Yang, X. (2016b). A brief review on the ecological network analysis with applications in the emerging medical ecology. In Hydrocarbon and Lipid Microbiology Protocols, Springer Protocols Handbooks, T. McGenity and et al., eds. (Springer), pp. 7–41.

Ning, D., Deng, Y., Tiedje, J.M., and Zhou, J. (2019). A general framework for quantitatively assessing ecological stochasticity. Proc. Natl. Acad. Sci. U S A *116*, 16892–16898.

Newman, M.E.J., and Clauset, A. (2016). Structure and inference in annotated networks. Nat. Commun. *7*, 11863.

Nowak, M.A. (2006). Evolutionary Dynamics: Exploring the Equations of Life (Belknap Press of Harvard University Press), p. 377.

Ohta, T. (2008) Molecular Evolution: Nearly Neutral Theory. Encyclopedia of Life Sciences.

Rastelli, M., Knauf, C., and Cani, P.D. (2018). Gut microbes and health: a focus on the mechanisms: linking microbes, obesity, and related disorders. Obesity *26*, 792–800, https://doi.org/10.1002/oby.22175.

Rosindell, J., Hubbell, S.P., and Etienne, R.S. (2011). The unified neutral theory of biodiversity and biogeography at age ten. Trends Ecol. Evol. *26*, 340–348.

Shekhtman, L.M., Bagrow, J.P., and Brockmann, D. (2014). Robustness of skeletons and salient features in networks. J. Complex Netw. https://doi.org/10.1093/comnet/cnt019.

Sobel, J.D. (1999). Is there a protective role for vaginal flora? Curr. Infect. Dis. Rep. *1*, 379–383.

Turner, P.V. (2018). The role of the gut microbiota on animal model reproducibility. Anim. Model. Exp. Med. *1*, 109–115, https://doi.org/10.1002/ame2.12022.

Vellend, M. (2010). Conceptual synthesis in community ecology. Q. Rev. Biol. *85*, 183–206.

Vellend, M. (2016). The Theory of Ecological Communities (Princeton University Press).

Vemuri, R., Sylvia, K.E., Klein, S.L., Forster, S.C., Plebanski, M., Eri, R., and Flanagan, K.L. (2019). The microgenderome revealed: sex differences in bidirectional interactions between the microbiota, hormones, immunity and disease susceptibility. Semin. Immunopathol. *41*, 265–275.

Vogelzang, A., Guerrini, M., Minato, N., and Fagarasan, S. (2018). Microbiota—an amplifier of autoimmunity. Curr. Opin. Immunol. *55*, 15–21.

Williams, B., Landay, A., and Presti, R.M. (2016). Microbiome alterations in HIV infection a review. Cell. Micobiol. *18*, 645–651.

Zaneveld, J.R., Mcminds, R., and Vega Thurber, R. (2017). Stress and stability: applying the Anna Karenina principle to animal microbiomes. Nat. Microbiol. *2*, 17121.

iScience, Volume *23*

Supplemental Information

Critical Network Structures and Medical Ecology Mechanisms Underlying Human Microbiome-Associated Diseases

Zhanshan (Sam) Ma

Supplemental Information

Supplemental Tables S1-S15 and Figures S1-S3

Table S1. Brief information of the 27 case studies on microbiome associated diseases (MADs). Related to the Transparent Methods and Figs 2-7.

Case No.	Sites	Disease	Treatments (Groups)	References* In "Transparent Methods" section
1	Gut	IBD (Inflammatory Bowel Disease)	Crohn's disease (CD) (18), Ulcerative colitis (UC) (38), Healthy (18)	Papa et al (2012)
2#@			CD (251), UC (324), Healthy (62)	Halfvarson et al (2017)
3		Obesity	Lean (61), Obese (196) and Overweight (24)	Turnbaugh et al (2009)
4		CRC	Cancer (46) vs. Healthy (56)	Wang et al (2012)
5#		HIV	Non-treatment (7) vs. ART treatment (11)	Neff et al (2018)
6			WithART(14), WithoutART(12), Healthy (22)	Lozupone et al (2013)
7			HIV Negative (20) *vs.* Positive (40)	McHardy et al (2013)
8#		Type 1 diabetes and Obesity	Normal T1D (33) vs Normal Healthy (33)	Kim, Jane: https://clinicaltrials.gov/ct2/show/NCT02938806
			Obesity T1D (24) vs. Obesity Healthy (26)	
9		Gout	Disease (41) vs. Healthy (42)	Guo et al (2015)
10		MHE	MHE (25), Cirrhotic (25), Healthy (25)	Zhang et al (2013)
11		Parkinson's Disease	Disease (205) vs. Healthy (133)	Hill-Burns et al 2017)
12		Schizophrenia	Disease (25). vs. Healthy (25)	Dilip Jeste (UC San Diego):https://profiles.ucsd.edu/dilip.jeste
13		Autism, Neurotypical	Autism (88), Neurotypical (41), Healthy (14)	Kang et al (2017)
14		Atherosclerosis	Disease (15) vs. Healthy (15)	Koren et al (2010)
15	Oral	Atherosclerosis	Disease (14) vs. Healthy (15)	Koren et al (2010)
16		Periodontitis	PB (22), PnB (22), Healthy (17)	Abusleme et al (2013)
17			Disease (29), Control (29), Healthy (29)	Griffen et al (2012)
18		Smoking	Smoking (6) vs. Non-smoking (9)	Lazarevic et al (2010)
19			Smoking (74) vs. Non-smoking (72)	Charlson et al (2010)
20	Nostril	Smoking	Smoking (74) vs. Non-smoking (71)	Charlson et al (2010)
21	Skin	Psoriasis	Disease (77), Control (83), Healthy (76)	Alekseyenko et al (2013)
22	Lung	Cystic Fibrosis (CF)	End of Treatment (23) vs. Exacerbation (23)	Fodor et al (2012)
23			Disease (16) vs. Healthy (10)	Blainey et al 2012)
24		HIV	Disease (82) vs. Healthy (77)	Lozupone et al (2013)
25	Vaginal	Bacterial Vaginosis (BV)	ABV, SBV, Healthy	Srinivasan et al. (2012)
26	Semen	Infertile	Abnormal (33), Subnormal (28), Normal (35). Genus level and species level	Weng et al 2014
27@	Milk	Mastitis	Mastitis (4) *vs*. Healthy (16)	Urbaniak (2015)

*These are the same datasets used in Ma, Li & Gotelli (2019) Diversity-disease relationships and shared species analyses for human microbiome-associated diseases. The ISME Journal, https://www.nature.com/articles/s41396-019-0395-y, where a brief description on the datasets can be found.
#: Case No. 2, 5 & 8 datasets were not used for neutral-theoretic analysis because of computational failures.
@: Case No 2 & 27 datasets were not used for core/periphery/skeleton nerwork analysis (computational failures).

*References (Cited in Table S1 for Data Sources)

Papa E, Docktor M, Smillie C, et al. 2012. Non-Invasive Mapping of the Gastrointestinal Microbiota Identifies Children with Inflammatory Bowel Disease. *Plos One*, 7(6):e39242.

Halfvarson J, Brislawn CJ, Lamendella R, et al. 2017. Dynamics of the human gut microbiome in Inflammatory Bowel Disease. *Nature Microbiology*, 2:17004.

Turnbaugh PJ, Hamady M, Yatsunenko T, et al. 2009. A core gut microbiome in obese and lean twins. *Nature*, 457(7228):480.

Wang T, Cai G, Qiu Y, et al. 2012. Structural segregation of gut microbiota between colorectal cancer patients and healthy volunteers. *The ISME Journal*, 6(2):320-329.

Neff CP, Krueger O, Xiong K, et al. 2018. Fecal Microbiota Composition Drives Immune Activation in HIV-infected Individuals. *Ebiomedicine*, 30.

Lozupone C, Cota-Gomez A, Palmer B E, et al. 2013. Widespread colonization of the lung by Tropheryma whipplei in HIV infection. *American Journal of Respiratory & Critical Care Medicine*, 187(10):1110-1117.

Mchardy IH, Li X, Tong M, et al. 2013. HIV Infection is associated with compositional and functional shifts in the rectal mucosal microbiota. *Microbiome*, 1(1):26.

Guo Z, Zhang J, Wang Z, et al. 2016. Intestinal Microbiota Distinguish Gout Patients from Healthy Humans. *Sci Rep*, 6:20602.

Zhang Z, Zhai H, Geng J, et al. 2013. Large-scale survey of gut microbiota associated with MHE Via 16S rRNA-based pyrosequencing. *American Journal of Gastroenterology,* 108(10):1601-1611.

Hill-Burns EM, Debelius JW, Morton JT et al. 2017. Parkinson's Disease and PD Medications Have Distinct Signatures of the Gut Microbiome. *Movement Disorders Official Journal of the Movement Disorder Society*, 32(5):739.

Kim, Jane: for Study Case No 8 in Table S1 https://clinicaltrials.gov/ct2/show/NCT02938806

Dilip Jeste (UC San Diego) for Study Case No 12 in Table S1: https://profiles.ucsd.edu/dilip.jeste

Kang DW, Adams JB, Gregory AC, et al. 2017. Microbiota Transfer Therapy alters gut ecosystem and improves gastrointestinal and autism symptoms: an open-label study. *Microbiome*, 5(1):10.

Koren O, Klaenhammer TR. 2011. Human oral, gut, and plaque microbiota in patients with atherosclerosis. *PNAS*, 108(Suppl 1):4592-4598.

Koren O, Klaenhammer TR. 2011. Human oral, gut, and plaque microbiota in patients with atherosclerosis. *PNAS*, 108(Suppl 1):4592-4598.

Abusleme L, Dupuy AK, Dutzan N, et al. 2013. The subgingival microbiome in health and periodontitis and its relationship with community biomass and inflammation. *The ISME Journal*, 7(5):1016-1025.

Griffen AL, Beall CJ, Campbell JH, et al. 2012. Distinct and complex bacterial profiles in human periodontitis and health revealed by 16S pyrosequencing. *The ISME Journal*, 6(6):1176.

Lazarevic V, Whiteson K, Hernandez D, et al. 2010. Study of inter- and intra-individual variations in the salivary microbiota. *BMC Genomics*, 11(1):1-11.

Charlson ES, Chen J, Custersallen R, et al. 2010. Disordered microbial communities in the upper respiratory tract of cigarette smokers. *Plos One*, 5(12):e15216.

Charlson ES, Chen J, Custersallen R, et al. 2010. Disordered microbial communities in the upper respiratory tract of cigarette smokers. *Plos One*, 5(12):e15216.

Alekseyenko AV, Perezperez GI, Souza AD, et al. 2013. Community differentiation of the cutaneous microbiota in psoriasis. *Microbiome*,1,1(2013-12-23), 1(1):31-31.

Fodor AA, Klem ER, Gilpin DF, et al. 2012. The Adult Cystic Fibrosis Airway Microbiota Is Stable over Time and Infection Type, and Highly Resilient to Antibiotic Treatment of Exacerbations. *Plos One*, 7(9):e45001.

Blainey PC, Milla CE, Cornfield DN, et al. 2012. Quantitative analysis of the human airway microbial ecology reveals a pervasive signature for cystic fibrosis. *Science Translational Medicine*, 4(153):153ra130.

Lozupone C, Cota-Gomez A, Palmer B E, et al. 2013. Widespread colonization of the lung by Tropheryma whipplei in HIV infection. *American Journal of Respiratory & Critical Care Medicine*, 187(10):1110-1117.

Srinivasan S, Hoffman NG, Morgan MT, et al. 2012. Bacterial Communities in Women with Bacterial Vaginosis: High Resolution Phylogenetic Analyses Reveal Relationships of Microbiota to Clinical Criteria. *Plos One*, 7(6):e37818.

Weng SL, Chiu CM, Lin FM, et al. 2014. Bacterial Communities in Semen from Men of Infertile Couples: Metagenomic Sequencing Reveals Relationships of Seminal Microbiota to Semen Quality. *Plos One*, 9(10):e110152.

Urbaniak C, Mcmillan A, Angelini M, et al. 2014. Effect of chemotherapy on the microbiota and metabolome of human milk, a case report. *Microbiome*, 2(1):24.

Table S3. The percentages (%) that passed neutrality test for Hubbell's classic neutral theory with the 24 datasets of the human MADs (Related to Fig 4)

Sites	Diseases	Treatments		Raw Community Data	Remove rarest species			
					Singleton	M1	M2	M3
Gut	IBD (Inflammatory Bowel Disease)	1	Healthy	22.22	11.11	77.78	83.33	66.67
			CD	27.78	5.56	83.33	77.78	72.22
			UC	65.79	44.74	84.21	81.58	71.05
	Obesity	2	Lean	0.00	0.00	65.57	85.25	83.61
			Overweight	4.17	0.00	83.33	83.33	79.17
			Obesity	2.06	0.52	58.76	77.84	81.35
	Cancer	3	Healthy	0.00	0.00	30.36	80.36	75.00
			Cancer	2.17	0.00	45.65	84.78	80.43
	HIV	4	Negative	0.00	0.00	90.48	100.00	100.00
			Treatment	21.43	21.43	100.00	100.00	100.00
			Non-treat	0.00	0.00	83.33	100.00	100.00
		5	Negative	NA	95.00	100.00	100.00	100.00
			Positive	100.00	100.00	100.00	100.00	100.00
	Gout	6	Healthy	38.10	26.19	97.62	100.00	97.62
			Gout	60.98	58.54	100.00	100.00	97.56
	MHE	7	Healthy	12.50	4.17	62.50	65.22	65.22
			Control	16.00	8.00	68.00	80.00	84.00
			MHE	4.17	8.33	70.83	83.33	79.17
	Parkinson's Disease	8	Healthy	89.47	33.08	97.74	96.24	93.98
			PD	88.29	26.47	98.53	95.07	95.57
	Schizophrenia	9	Healthy	12.00	8.00	92.00	100.00	100.00
			Disease	12.00	20.00	100.00	100.00	100.00
	Autism	10	Healthy	92.86	50.00	85.71	85.71	78.57
			Autism	95.45	53.41	94.32	95.45	92.05
			Neurotypical	97.56	73.17	100.00	95.12	95.12
	Atherosclerosis	11	Healthy	0.00	0.00	0.00	46.67	53.33
			Disease	0.00	0.00	6.67	53.33	60.00
Oral	Atherosclerosis	12	Healthy	73.33	26.67	86.67	93.33	93.33
			Disease	42.86	14.29	100.00	100.00	100.00
	Periodontitis	13	Healthy	82.35	52.94	94.12	82.35	82.35
			PB	63.64	18.18	77.27	63.64	68.18
			PnB	40.91	18.18	77.27	77.27	59.09
		14	Healthy	3.45	0.00	17.24	13.79	20.69
			Control	10.34	0.00	20.69	10.34	13.79
			Disease	3.45	0.00	6.90	0.00	6.90
	Smoking	15	Non-Smoker	0.00	0.00	55.56	88.89	77.78
			Smoker	0.00	0.00	100.00	100.00	100.00
		16	Non-Smoker	26.76	38.03	92.96	97.18	94.37
			Smoker	6.85	15.07	87.67	91.78	86.30
		17	Non-Smoker	22.22	0.00	83.33	76.39	72.22
			Smoker	19.18	4.17	69.44	68.06	63.89
Skin	Psoriasis	18	Control	7.23	2.41	32.53	73.49	85.54
			Normal	3.95	1.32	32.89	63.16	73.68

			Lesion	6.49	1.30	40.26	71.43	81.82
Lung	Cystic Fibrosis	19	Treated	100.00	95.45	100.00	95.45	95.24
			Exacerbation	100.00	96.00	100.00	95.65	100.00
		20	Healthy	44.44	11.11	66.67	66.67	55.56
			Disease	56.25	31.25	68.75	68.75	37.50
	HIV	21	Negative	68.42	44.26	78.69	75.00	68.33
			Positive	75.56	53.33	88.89	88.89	84.44
Vaginal	BV	22	Healthy	99.03	95.60	95.60	92.21	93.07
			BV	76.92	47.41	67.24	56.52	49.57
Semen	Infertile (Species level)	23	Normal	8.57	2.86	31.43	62.86	74.29
			Subnormal	0.00	0.00	35.71	75.00	89.29
			Abnormal	0.00	0.00	30.30	66.67	72.73
Milk	Mastitis	24	Healthy	93.75	100.00	100.00	100.00	100.00
			Mastitis	100.00	100.00	100.00	75.00	75.00
Passing Percentages (%)			Health	35.65	26.16	68.75	78.29	77.71
			Diseased	39.13	27.05	75.29	80.88	79.28

Table S4. The *p*-value of Fisher's exact test for the numbers of samples passing the neutrality test between the healthy and diseased datasets (Related to Figs 2-3)

Microbiome	Disease	Index	Healthy	Diseased	Raw Community Data	Remove rarest species			
						Singleton	M1	M2	M3
Gut	IBD (Inflammatory Bowel Disease)	1	Healthy	CD	1.000	1.000	1.000	1.000	1.000
			Healthy	UC	0.075	0.078	1.000	1.000	1.000
	Obesity	2	Lean	Overweight	0.291	1.000	0.583	1.000	1.000
			Lean	Obesity	0.576	1.000	0.638	0.744	0.913
	Cancer	3	Healthy	Cancer	0.456	1.000	0.343	0.883	0.881
	HIV	4	Negative	Treatment	0.081	0.081	1.000	1.000	1.000
			Negative	Non-treatment	1.000	1.000	1.000	1.000	1.000
		5	Negative	Positive	NA	1.000	1.000	1.000	1.000
	Gout	6	Healthy	Gout	0.255	0.069	1.000	1.000	1.000
	MHE	7	Healthy	Control	1.000	1.000	1.000	0.663	0.660
			Healthy	MHE	0.611	1.000	0.823	0.657	0.822
	Parkinson's Disease	8	Healthy	PD	0.936	0.352	1.000	1.000	0.936
	Schizophrenia	9	Healthy	Schizophrenia	1.000	0.427	0.843	1.000	1.000
	Autism	10	Healthy	Autism	1.000	1.000	0.837	0.836	0.831
			Healthy	Neurotypical	1.000	0.614	0.823	1.000	0.819
	Atherosclerosis	11	Healthy	Atheroscierosis	1.000	1.000	1.000	1.000	1.000
Oral	Atherosclerosis	12	Healthy	Atheroscierosis	0.540	0.666	1.000	1.000	1.000
	Periodontitis	13	Healthy	PB	0.628	0.199	0.813	0.628	0.807
			Healthy	PnB	0.293	0.199	0.813	1.000	0.618
		14	Healthy	Control	0.613	1.000	1.000	1.000	0.735
			Healthy	Disease	1.000	1.000	0.430	0.116	0.265
	Smoking	15	Non-smoking	Smoking	1.000	1.000	0.692	1.000	1.000
		16	Non-smoking	Smoking	0.008	0.018	0.904	0.905	0.718
		17	Non-smoking	Smoking	0.841	0.245	0.527	0.700	0.695
Skin	Psoriasis	18	Control	Lesion	1.000	1.000	0.541	1.000	0.907
			Normal	Lesion	0.720	1.000	0.536	0.702	0.714
Lung	Cystic Fibrosis (CF)	19	End of Treatment	Exacerbation	1.000	1.000	1.000	1.000	1.000
		20	Healthy	CF	1.000	0.634	1.000	1.000	0.716
	HIV	21	Negative	Positive	0.836	0.610	0.771	0.660	0.550
Vaginal	BV	22	Healthy	BV	0.236	0.002	0.096	0.033	0.004
Semen	Infertile (Species level)	23	Normal	Subnormal	0.256	1.000	0.806	0.695	0.707
			Normal	Abnormal	0.243	1.000	1.000	1.000	1.000
Milk	Mastitis	24	Healthy	Mastitis	1.000	1.000	1.000	1.000	1.000

Table S5. The *p*-values of the permutation tests for the differences in the neutral theory parameters between the healthy and diseased datasets (Related to Figs 2-3)

Micro-biome	Disease	Index	Healthy	Diseased	Raw Community Data		Remove rarest species							
							Singleton		M1		M2		M3	
					θ	m	θ	m	θ	m	θ	m	θ	m
	IBD (Inflammatory Bowel Disease)	1	Healthy	CD	0.542	0.839	0.563	0.239	0.628	0.888	0.815	0.501	0.791	0.406
			Healthy	UC	0.001	0.308	0.000	0.938	0.000	0.993	0.001	0.572	0.002	0.658
	Obesity	2	Lean	Overweight	0.722	0.926	0.707	0.322	0.657	0.030	0.693	0.671	0.650	0.957
			Lean	Obesity	0.081	0.123	0.246	0.408	0.313	0.048	0.225	0.080	0.179	0.493
	Cancer	3	Healthy	Cancer	0.000	0.062	0.043	0.359	0.042	0.827	0.076	0.699	0.321	0.508
	HIV	4	Negative	Treatment	0.052	1.000	0.096	0.325	0.127	0.414	0.175	0.702	0.263	0.606
			Negative	Non-treatment	0.811	0.782	0.471	0.427	0.385	0.699	0.326	0.242	0.274	0.044
		5	Negative	Positive	NA	NA	0.694	0.650	0.460	0.994	0.408	0.866	0.735	0.506
	Gout	6	Healthy	Gout	0.001	0.641	0.001	0.680	0.001	0.401	0.002	0.106	0.003	0.381
	MHE	7	Healthy	Control	0.073	0.670	0.278	0.154	0.132	0.356	0.226	0.653	0.335	0.057
			Healthy	MHE	0.301	0.153	0.255	0.273	0.147	0.959	0.025	0.124	0.028	0.001
	Parkinson's Disease	8	Healthy	PD	0.084	0.149	0.118	0.736	0.077	0.234	0.118	0.471	0.135	0.718
	Schizophrenia	9	Healthy	Schizophrenia	0.307	0.848	0.464	0.832	0.453	0.095	0.397	0.715	0.407	0.788
	Autism	10	Healthy	Autism	0.314	0.487	0.283	0.163	0.300	0.305	0.343	0.842	0.481	0.789
			Healthy	Neurotypical	0.626	0.667	0.695	0.886	0.738	0.626	0.826	0.547	0.782	0.977
	Atherosclerosis	11	Healthy	Atherosclerosis	0.595	0.267	0.775	0.137	0.775	0.217	0.838	0.217	0.870	0.461
Oral	Atherosclerosis	12	Healthy	Atherosclerosis	0.033	0.780	0.026	0.290	0.023	0.780	0.041	0.158	0.026	0.093
	Periodontitis	13	Healthy	PB	0.000	0.604	0.000	0.006	0.000	0.027	0.000	0.333	0.000	0.039
			Healthy	PnB	0.002	0.077	0.000	0.012	0.000	0.408	0.000	0.110	0.001	0.029
		14	Healthy	Control	0.013	0.362	0.012	0.210	0.014	0.265	0.013	0.307	0.008	0.330
			Healthy	Disease	0.000	0.163	0.000	0.163	0.000	0.215	0.000	0.345	0.000	0.353
	Smoking	15	Non-smoking	Smoking	0.607	0.456	0.328	0.088	0.388	0.005	0.689	0.776	0.864	0.272
		16	Non-smoking	Smoking	0.001	0.007	0.055	0.092	0.073	0.842	0.153	0.297	0.057	0.012
		17	Non-smoking	Smoking	0.138	0.100	0.091	0.511	0.069	0.337	0.442	0.790	0.534	0.285
Skin	Psoriasis	18	Control	Lesion	0.889	0.017	0.774	0.040	0.962	0.038	0.951	0.004	0.967	0.348
			Normal	Lesion	0.548	0.937	0.616	0.676	0.789	0.949	0.578	0.811	0.432	0.932
Lung	Cystic Fibrosis (CF)	19	End of Treatment	Exacerbation	0.074	0.195	0.492	1.000	0.453	0.992	0.227	0.411	0.363	0.442
		20	Healthy	CF	0.000	0.388	0.000	0.207	0.000	0.251	0.049	0.032	0.049	0.037
	HIV	21	Negative	Positive	0.286	0.422	0.697	0.486	0.645	0.730	0.828	0.571	0.843	0.571
Vaginal	BV	22	Healthy	BV	0.000	0.000	0.000	0.000	0.000	0.000	0.000	0.000	0.000	0.000
Semen	Infertile (Species level)	23	Normal	Subnormal	0.550	0.437	0.429	0.645	0.470	0.645	0.462	0.174	0.268	0.726
			Normal	Abnormal	0.705	0.922	0.592	0.542	0.617	0.212	0.464	0.271	0.335	0.145
Milk	Mastitis	24	Healthy	Mastitis	0.494	0.554	1.000	0.800	0.800	0.533	1.000	0.800	0.374	0.304
Significant difference rate (%)					33.33	9.09	30.30	12.12	30.30	18.18	30.30	9.09	30.30	21.21

Table S7. The shared core/periphery analysis between the healthy and diseased treatments based on the 1000 sets of permutated core/periphery networks (CPN) built with FDR control and p=0.001 (Related to Figs 6-7)

Microbiome	Disease	Index	Healthy	Diseased	Core			Periphery		
					Obs.	Perm.	*p-value*	Obs.	Perm.	*p-value*
Gut	IBD (Inflammatory Bowel Disease)	1	Healthy	CD	1	1.618	0.545	7	9.674	0.282
			Healthy	UC	1	0.900	0.776	9	6.196	0.898
	Obesity	3	Lean	Overweight	1	1.895	0.505	12	7.495	0.932
			Lean	Obesity	10	9.781	0.597	23	20.753	0.720
	Cancer	4	Healthy	Cancer	9	11.796	0.249	11	15.48	0.160
	HIV	5	Negative	Treatment	22	28.498	0.178	43	37.691	0.792
			Negative	Non-treatment	24	25.658	0.456	27	30.546	0.357
		6	Negative	Treatment	15	26.606	0.029	25	33.909	0.107
			Negative	Non-treatment	11	26.427	0.002	23	32.571	0.106
		7	Negative	Positive	22	13.173	0.957	18	18.304	0.541
	T1D (Lean)	8	Healthy	T1D	10	8.496	0.763	19	16.18	0.792
	T1D (Obesity)		Healthy	T1D	20	15.005	0.902	28	24.807	0.760
	Gout	9	Healthy	Gout	1	5.43	0.035	17	17.809	0.492
	MHE	10	Healthy	MHE	6	4.86	0.772	6	13.842	0.026
			Control	MHE	3	4.702	0.342	12	13.68	0.427
	Parkinson's Disease	11	Healthy	PD	38	45.7	0.170	40	47.696	0.177
	Schizophrenia	12	Healthy	Schizophrenia	30	29.815	0.547	26	34.969	0.077
	Autism	13	Healthy	Autism	3	1.97	0.865	9	6.978	0.768
			Healthy	Neurotypical	0	0.706	0.679	4	4.875	0.580
	Atherosclerosis	14	Healthy	Atherosclerosis	29	27.573	0.671	23	30.778	0.102
Oral	Atherosclerosis	15	Healthy	Atherosclerosis	0	0.523	0.589	2	4.616	0.170
	Periodontitis	16	Healthy	PB	1	0.592	0.865	2	4.145	0.257
			Healthy	PnB	0	0.619	0.605	2	3.978	0.266
		17	Healthy	Disease	15	6.815	0.928	14	6.387	0.939
			Control	Disease	0	6.799	0.092	0	6.244	0.085
	Smoking	18	Non-smoking	Smoking	4	2.368	0.887	13	14.387	0.438
		19	Non-smoking	Smoking	20	34.991	0.019	20	34.701	0.008
		20	Non-smoking	Smoking	0	0.957	0.522	16	11.421	0.905
Skin	Psoriasis	21	Control	Lesion	84	112.266	0.014	94	116.43	0.032
			Normal	Lesion	109	105.23	0.644	106	110.03	0.393
Lung	Cystic Fibrosis (CF)	22	End of Treatment	Exacerbation	0	8.69	0.011	0	27.068	0.000
		23	Healthy	CF	0	0.549	0.644	1	2.016	0.447
	HIV	24	Negative	Positive	181	168.219	0.605	118	105.99	0.741
Vaginal	BV	25	Healthy	BV	0	13.183	0.003	0	23.395	0.000
Semen	Infertile (Genus level)	26	Normal	Subnormal	1	59.733	0.000	0	57.235	0.000
			Normal	Abnormal	0	63.879	0.000	4	58.901	0.000
	Infertile Species level)		Normal	Subnormal	69	64.506	0.658	63	67.569	0.378
			Normal	Abnormal	67	65.134	0.584	51	69.039	0.066
Percentage of Comparisons with Reduced Shared Skeletons					23.68% (9/38)			18.42% (7/38)		
Percentage of Comparisons without the change					76.32% (29/38)			81.58% (31/38)		

*Obs.=The Observed value. Perm.=The mean value from 1000 permutated networks. p-value is from permutation test.

Table S8. The *p*-values from the permutation test for the differences in the core/periphery network (CPN) properties between the H (healthy) & D (diseased) treatments with 1000 sets of permutated CPNs (*p*-value<0.05, indicating significant difference) (Related to Figs 6-7)

Microbiome	Disease	Index	Healthy	Diseased	ρ	C/ (C+P)	B11	B12 (21)	B22	Nestedness (S)
Gut	IBD (Inflammatory Bowel Disease)	1	Healthy	CD	0.00	0.00	0.00	1.00	0.00	1.00
			Healthy	UC	0.00	1.00	1.00	0.00	0.00	0.00
	Obesity	3	Lean	Overweight	0.00	0.00	0.00	1.00	1.00	0.00
			Lean	Obesity	0.00	0.00	0.00	1.00	0.00	0.00
	Cancer	4	Healthy	Cancer	0.00	0.00	0.00	0.00	0.00	0.00
	HIV	5	Negative	Treatment	0.00	0.00	0.00	0.00	1.00	0.00
			Negative	Non-treatment	1.00	1.00	1.00	0.00	0.00	0.00
		6	Negative	Treatment	0.00	1.00	0.00	0.00	0.00	0.00
			Negative	Non-treatment	1.00	0.00	1.00	1.00	0.00	1.00
		7	Negative	Positive	0.00	1.00	0.00	0.00	1.00	0.00
	T1D (Lean)	8	Healthy	T1D	0.00	0.00	0.00	0.00	0.00	0.00
	T1D (Obesity)		Healthy	T1D	1.00	1.00	0.00	0.00	0.00	0.00
	Gout	9	Healthy	Gout	1.00	1.00	1.00	0.00	0.00	1.00
	MHE	10	Healthy	MHE	1.00	1.00	1.00	0.00	0.00	1.00
			Control	MHE	1.00	1.00	1.00	0.00	1.00	1.00
	Parkinson's Disease	11	Healthy	PD	0.00	0.00	0.00	0.00	0.00	0.00
	Schizophrenia	12	Healthy	Schizophrenia	0.00	0.00	1.00	1.00	1.00	1.00
	Autism	13	Healthy	Autism	1.00	1.00	1.00	1.00	0.00	1.00
			Healthy	Neurotypical	1.00	1.00	1.00	1.00	0.00	1.00
	Atherosclerosis	14	Healthy	Atherosclerosis	1.00	1.00	1.00	1.00	0.00	1.00
Oral	Atherosclerosis	15	Healthy	Atherosclerosis	0.00	0.00	0.00	1.00	0.00	0.00
	Periodontitis	16	Healthy	PB	1.00	1.00	0.00	1.00	1.00	1.00
			Healthy	PnB	0.00	0.00	0.00	1.00	1.00	0.00
		17	Healthy	Disease	0.00	1.00	0.00	0.00	0.00	0.00
			Control	Disease	0.00	1.00	1.00	1.00	0.00	1.00
	Smoking	18	Non-smoking	Smoking	1.00	1.00	1.00	1.00	1.00	1.00
		19	Non-smoking	Smoking	0.00	1.00	0.00	0.00	0.00	0.00
		20	Non-smoking	Smoking	1.00	0.00	1.00	0.00	1.00	1.00
Skin	Psoriasis	21	Control	Lesion	0.00	1.00	1.00	1.00	1.00	0.00
			Normal	Lesion	0.00	1.00	1.00	0.00	0.00	0.00
Lung	Cystic Fibrosis (CF)	22	End of Treatment	Exacerbation	0.00	0.00	1.00	1.00	0.00	0.00
		23	Healthy	CF	1.00	1.00	1.00	1.00	0.00	0.00
	HIV	24	Negative	Positive	0.00	1.00	0.00	0.00	0.00	0.00
Vaginal	BV	25	Healthy	BV	0.00	0.00	0.00	1.00	0.00	0.00
Semen	Infertile (Genus level)	26	Normal	Subnormal	0.00	1.00	0.00	1.00	0.00	0.00
			Normal	Abnormal	0.00	0.00	1.00	1.00	0.00	0.00
	Infertile Species level)		Normal	Subnormal	0.00	1.00	0.00	0.00	0.00	0.00
			Normal	Abnormal	1.00	1.00	1.00	1.00	1.00	1.00
Percentage of Significant Differences (%)					59.18	44.90	51.02	46.94	63.27	57.14

Here the algorithm for permutation test is as follows:
OP=|Observed Property Difference between H & D|
PP=1000 values of |H-D| from permutated networks
N=number of permutations satisfying PP≤OP
Pseudo-P-value=N/1000

Table S9. The shared skeleton analysis between the healthy and diseased treatments based on the 1000 sets of permutated high-salience skeleton networks (HSNs) built with FDR control and p=0.001 (HSS>0) (Related to Figs 6-7)

Microbiome	Disease	Index	Healthy	Diseased	HSS (High Salience Skeleton) Value>0		
					Obs.	**P**erm.	***p**-value*
Gut	IBD (Inflammatory Bowel Disease)	1	Healthy	CD	49	143.27	0.111
			Healthy	UC	80	55.44	0.785
	Obesity	3	Lean	Overweight	166	111.85	0.803
			Lean	Obesity	1132	1072.96	0.605
	Cancer	4	Healthy	Cancer	630	1185.00	0.026
	HIV	5	Negative	Treatment	NA	NA	NA
			Negative	Non-treatment	NA	NA	NA
		6	Negative	Treatment	2718	6057.995	0.007
			Negative	Non-treatment	1934	5855.577	0.003
		7	Negative	Positive	2049	1495.90	0.839
	T1D (Lean)	8	Healthy	T1D	1059	923.64	0.720
	T1D (Obesity)		Healthy	T1D	3393	2411.57	0.965
	Gout	9	Healthy	Gout	407	748.53	0.046
	MHE	10	Healthy	MHE	172	489.41	0.041
			Control	MHE	309	478.13	0.206
	Parkinson's Disease	11	Healthy	PD	3630	6724.11	0.015
	Schizophrenia	12	Healthy	Schizophrenia	4861	6664.09	0.067
	Autism	13	Healthy	Autism	43	89.80	0.425
			Healthy	Neurotypical	24	46.23	0.662
	Atherosclerosis	14	Healthy	Atherosclerosis	4288	5592.62	0.083
Oral	Atherosclerosis	15	Healthy	Atherosclerosis	2	26.69	0.031
	Periodontitis	16	Healthy	PB	1	23.57	0.057
			Healthy	PnB	1	23.11	0.047
		17	Healthy	Disease	1353	441.901	0.944
			Control	Disease	0	437.733	0.043
	Smoking	18	Non-smoking	Smoking	279	353.64	0.388
		19	Non-smoking	Smoking	1707	4029.50	0.029
		20	Non-smoking	Smoking	153	147.17	0.577
Skin	Psoriasis	21	Control	Lesion	37098	62519.264	0.002
			Normal	Lesion	64145	55303.513	0.833
Lung	Cystic Fibrosis (CF)	22	End of Treatment	Exacerbation	0	456.75	0.000
		23	Healthy	CF	0	6.78	0.202
	HIV	24	Negative	Positive	19746	33750.779	0.346
Vaginal	BV	25	Healthy	BV	0	23.359	0.000
Semen	Infertile (Genus level)	26	Normal	Subnormal	3	654.33	0.000
			Normal	Abnormal	6	561.187	0.000
	Infertile Species level)		Normal	Subnormal	26291	29221.901	0.402
			Normal	Abnormal	24225	29292.624	0.249
Percentage of Comparisons with Reduced Shared Skeletons					39.47%(15/38)		
Percentage of Comparisons without the change					60.53%(23/38)		

*In general, the observed shared skeletons (*OSS*) should be smaller or, at most, equal with the permutated shared skeletons (*PSS*), *i.e.*, $OSS \leq PSS$. In other words, the case of $O>P$ is unlikely and corresponding p-value would be p=1.

Table S10. The *p*-values from the permutation test for the differences in the high salience skeleton network (HSN) properties between the H & D treatments with 1000 sets of permutated HSNs (*p* value<0.05, indicating significant difference) (Related to Figs 6-7)

Microbiome	Disease	Index	Healthy	Diseased	Links (%)	Max	Skewness	Kurtosis	r_{HSS}
Gut	IBD (Inflammatory Bowel Disease)	1	Healthy	CD	1.00	0.00	1.00	0.00	0.00
			Healthy	UC	1.00	0.00	1.00	1.00	0.00
	Obesity	3	Lean	Overweight	1.00	1.00	1.00	0.00	0.00
			Lean	Obesity	0.00	0.00	0.00	0.00	0.00
	Cancer	4	Healthy	Cancer	0.00	0.00	1.00	1.00	0.00
	HIV	5	Negative	Treatment	0.00	0.00	1.00	1.00	0.00
			Negative	Non-treatment	0.00	0.00	1.00	0.00	0.00
		6	Negative	Treatment	0.00	0.00	0.00	0.00	0.00
			Negative	Non-treatment	0.00	1.00	0.00	1.00	0.00
		7	Negative	Positive	1.00	1.00	1.00	0.00	0.00
	T1D (Lean)	8	Healthy	T1D	1.00	1.00	1.00	0.00	1.00
	T1D (Obesity)		Healthy	T1D	0.00	0.00	1.00	1.00	1.00
	Gout	9	Healthy	Gout	0.00	0.00	1.00	1.00	1.00
	MHE	10	Healthy	MHE	1.00	0.00	1.00	1.00	0.00
			Control	MHE	0.00	1.00	0.00	0.00	0.00
	Parkinson's Disease	11	Healthy	PD	0.00	0.00	1.00	1.00	0.00
	Schizophrenia	12	Healthy	Schizophrenia	0.00	0.00	0.00	0.00	0.00
	Autism	13	Healthy	Autism	0.00	0.00	0.00	0.00	0.00
			Healthy	Neuro-typical	1.00	1.00	0.00	0.00	1.00
	Atherosclerosis	14	Healthy	Atherosclerosis	0.00	0.00	0.00	0.00	0.00
Oral	Atherosclerosis	15	Healthy	Atherosclerosis	1.00	0.00	1.00	1.00	0.00
	Periodontitis	16	Healthy	PB	0.00	0.00	0.00	0.00	0.00
			Healthy	PnB	0.00	0.00	1.00	1.00	0.00
		17	Healthy	Disease	1.00	1.00	0.00	0.00	0.00
			Control	Disease	1.00	1.00	0.00	0.00	0.00
	Smoking	18	Non-smoking	Smoking	1.00	1.00	1.00	0.00	1.00
		19	Non-smoking	Smoking	0.00	0.00	0.00	0.00	1.00
		20	Non-smoking	Smoking	1.00	1.00	1.00	1.00	1.00
Skin	Psoriasis	21	Control	Lesion	0.00	1.00	1.00	1.00	0.00
			Normal	Lesion	1.00	1.00	0.00	0.00	1.00
Lung	Cystic Fibrosis (CF)	22	End of Treatment	Exacerbation	1.00	0.00	1.00	1.00	0.00
		23	Healthy	CF	0.00	0.00	0.00	0.00	1.00
	HIV	24	Negative	Positive	0.00	0.00	0.00	0.00	0.00
Vaginal	BV	25	Healthy	BV	0.00	0.00	0.00	0.00	0.00
Semen	Infertile (Genus level)	26	Normal	Subnormal	1.00	0.00	0.00	0.00	0.00
			Normal	Abnormal	1.00	0.00	0.00	0.00	0.00
	Infertile Species level)		Normal	Subnormal	1.00	1.00	1.00	1.00	1.00
			Normal	Abnormal	1.00	0.00	1.00	0.00	0.00
% With significant differences					52.63	65.79	47.37	63.16	73.68

Table S11. The *observed* core/periphery parameters in the core-periphery networks for the 25 MAD (microbiome associated disease) datasets with FDR control and *p*-value=0.001 (Related to Figs 6-7)

Sites	Diseases	Treatments		*r*	C/(C+P)	Density Matrix			Nestedness (S)
						B11	B12 (21)	B22	
Gut	IBD (Inflammatory Bowel Disease)	1	Healthy	0.179	0.310	0.098	0.001	0.022	0.020
			CD	0.254	0.174	0.210	0.000	0.016	0.018
			UC	0.246	0.344	0.119	0.003	0.014	0.021
	Obesity	3	Lean	0.405	0.250	0.277	0.004	0.013	0.026
			Overweight	0.236	0.283	0.129	0.007	0.012	0.019
			Obesity	0.042	0.478	0.012	0.004	0.005	0.009
	Cancer	4	Healthy	0.027	0.470	0.006	0.002	0.003	0.003
			Cancer	0.079	0.406	0.021	0.003	0.004	0.006
	HIV	5	Negative	0.074	0.459	0.019	0.003	0.005	0.007
			Treatment	0.104	0.498	0.031	0.006	0.004	0.012
			Non-treatment	0.086	0.465	0.028	0.007	0.006	0.011
		6	Negative	0.117	0.446	0.039	0.007	0.006	0.013
			Treatment	0.082	0.442	0.026	0.005	0.007	0.010
			Non-treatment	0.091	0.413	0.034	0.007	0.008	0.012
		7	Negative	0.180	0.444	0.066	0.006	0.007	0.018
			Positive	0.064	0.434	0.017	0.003	0.006	0.007
	T1D (Lean)	8	Normal-Healthy	0.098	0.426	0.029	0.003	0.007	0.009
			Normal-T1D	0.068	0.480	0.018	0.003	0.007	0.007
	T1D (Obesity)		Obesity-Healthy	0.068	0.465	0.016	0.002	0.006	0.006
			Obesity-T1D	0.068	0.469	0.020	0.004	0.008	0.009
	Gout	9	Healthy	0.178	0.411	0.071	0.006	0.010	0.018
			Gout	0.118	0.436	0.041	0.004	0.011	0.013
	MHE	10	Healthy	0.174	0.310	0.081	0.005	0.011	0.015
			Control	0.182	0.345	0.087	0.006	0.014	0.019
			MHE	0.225	0.287	0.120	0.003	0.014	0.018
	Parkinson's Disease	11	Healthy	0.083	0.429	0.023	0.004	0.005	0.013
			PD	0.037	0.507	0.008	0.003	0.003	0.007
	Schizophrenia	12	Healthy	0.058	0.490	0.017	0.005	0.005	0.008
			Disease	0.059	0.460	0.018	0.005	0.006	0.008
	Autism	13	Healthy	0.301	0.331	0.218	0.013	0.030	0.043
			Autism	0.176	0.345	0.075	0.005	0.010	0.023
			Neurotypical	0.187	0.374	0.086	0.004	0.017	0.021
	Atherosclerosis	14	Healthy	0.054	0.483	0.015	0.004	0.006	0.007
			Disease	0.039	0.500	0.012	0.004	0.006	0.006
Oral	Atherosclerosis	15	Healthy	0.430	0.218	0.470	0.000	0.043	0.047
			Disease	0.164	0.340	0.076	0.000	0.019	0.017
	Periodontitis	16	Healthy	0.336	0.255	0.286	0.000	0.035	0.037
			PB	0.186	0.289	0.128	0.000	0.032	0.027
			PnB	0.612	0.136	1.000	0.000	0.034	0.042
		17	Healthy	0.113	0.496	0.153	0.068	0.093	0.095
			Control	0.027	0.518	0.032	0.023	0.021	0.025
			Disease	0.013	0.513	0.021	0.024	0.029	0.024
	Smoking	18	Non-Smoker	0.187	0.378	0.114	0.016	0.023	0.032
			Smoker	0.296	0.383	0.205	0.017	0.031	0.049
		19	Non-Smoker	0.170	0.391	0.082	0.011	0.012	0.037
			Smoker	0.094	0.437	0.032	0.006	0.008	0.019
		20	Non-Smoker	0.382	0.206	0.324	0.001	0.020	0.031
			Smoker	0.491	0.188	0.431	0.006	0.013	0.030
Skin	Psoriasis	21	Control	0.036	0.497	0.010	0.004	0.003	0.007
			Normal	0.032	0.491	0.008	0.003	0.003	0.006

			Lesion	0.028	0.501	0.008	0.004	0.003	0.007
Lung	Cystic Fibrosis	22	Treated	0.000	1.000	1.000	0.000	0.000	1.000
			Exacerbation	0.471	0.250	1.000	0.000	0.200	0.143
		23	Healthy	0.681	0.207	1.000	0.000	0.063	0.076
			Disease	0.608	0.167	1.000	0.000	0.053	0.061
	HIV	24	Negative	0.089	0.496	0.050	0.020	0.012	0.045
			Positive	0.188	0.495	0.146	0.045	0.024	0.090
Vaginal	BV	25	Healthy	0.387	0.353	0.400	0.000	0.109	0.092
			BV	0.632	0.500	1.000	0.000	1.000	0.333
Semen	Infertile (Genus level)	26	Normal	0.326	0.250	0.400	0.000	0.076	0.066
			Subnormal	0.625	0.227	1.000	0.000	0.103	0.104
			Abnormal	0.348	0.214	0.400	0.000	0.048	0.045
	Infertile (Species level)		Normal	0.051	0.501	0.014	0.005	0.004	0.007
			Subnormal	0.082	0.461	0.027	0.007	0.005	0.011
			Abnormal	0.049	0.488	0.016	0.007	0.005	0.008
Healthy		**Mean**		0.175	0.419	0.178	0.010	0.023	0.051
		Standard Error		0.026	0.020	0.042	0.003	0.004	0.022
Diseased		**Mean**		0.216	0.374	0.238	0.006	0.052	0.037
		Standard Error		0.033	0.020	0.060	0.001	0.028	0.010

Table S12. The *observed* statistical network properties of the high-salience skeleton networks for the 25 MAD (microbiome associated disease) datasets with FDR control and *p*-value=0.001 (Related to Figs 6-7)

Sites	Diseases	Treatments		Statistics of HSS						Assortativity
				Links (%)	Max	Mean	Std. Error	Skewness	Kurtosis	r_{HSS}
Gut	IBD (Inflammatory Bowel Disease)	1	Healthy	99.985	0.026	0.017	0.000	-33.349	3334.500	-0.009
			CD	99.945	0.035	0.023	0.001	-17.459	911.999	-0.012
			UC	99.984	0.019	0.013	0.000	-31.949	3059.750	-0.006
	Obesity	3	Lean	99.948	0.026	0.013	0.000	-7.085	973.275	-0.007
			Overweight	99.994	0.016	0.011	0.000	-53.842	8695.000	-0.005
			Obesity	73.168	0.519	0.004	0.020	22.358	519.682	-0.002
	Cancer	4	Healthy	99.992	0.008	0.003	0.000	29.987	8911.597	-0.002
			Cancer	100.000	0.004	0.004	0.000	0.000	0.000	-0.002
	HIV	5	Negative	99.959	0.015	0.003	0.000	50.530	5104.754	-0.002
			Treatment	99.998	0.005	0.002	0.000	-72.261	24815.977	-0.001
			Non-treat	99.950	0.017	0.002	0.000	54.377	5780.542	-0.001
		6	Negative	99.995	0.007	0.004	0.000	-48.101	10994.593	-0.002
			Treatment	99.999	0.007	0.004	0.000	-129.184	50063.500	-0.002
			Non-treat	99.999	0.007	0.004	0.000	-129.184	50063.500	-0.002
		7	Negative	99.995	0.010	0.005	0.000	-37.779	9847.053	-0.003
			Positive	99.973	0.015	0.006	0.000	-3.581	2036.490	-0.003
	T1D (Lean)	8	Normal-Healthy	99.998	0.010	0.007	0.000	-87.327	22876.000	-0.003
			Normal-T1D	99.996	0.010	0.007	0.000	-62.362	11664.500	-0.003
	T1D (Obesity)		Obesity-Healthy	100.000	0.006	0.006	0.000	0.000	0.000	-0.003
			Obesity-T1D	99.998	0.008	0.006	0.000	-103.204	31951.000	-0.003
	Gout	9	Healthy	99.949	0.030	0.008	0.000	27.417	3262.266	-0.004
			Gout	99.986	0.017	0.008	0.000	-6.210	3660.833	-0.004
	MHE	10	Healthy	100.000	0.010	0.010	0.000	0.000	0.000	-0.005
			Control	99.996	0.014	0.009	0.000	-63.368	12044.500	-0.005
			MHE	100.000	0.013	0.013	0.000	0.000	0.000	-0.007
	Parkinson's Disease	11	Healthy	88.116	0.332	0.005	0.012	22.326	540.969	-0.003
			PD	59.691	0.638	0.003	0.024	24.250	610.921	-0.001
	Schizophrenia	12	Healthy	100.000	0.004	0.004	0.000	0.000	0.000	-0.002
			Disease	99.999	0.005	0.004	0.000	-114.004	38988.500	-0.002
	Autism	13	Healthy	99.992	0.019	0.013	0.000	-45.183	6122.500	-0.006
			Autism	91.270	0.301	0.009	0.013	18.661	378.342	-0.004
			Neurotypical	99.947	0.040	0.011	0.000	16.341	2387.524	-0.006
	Atherosclerosis	14	Healthy	99.999	0.006	0.004	0.000	-141.020	59657.500	-0.002
			Disease	99.999	0.005	0.004	0.000	-163.247	79947.000	-0.002
Oral	Atherosclerosis	15	Healthy	100.000	0.036	0.036	0.000	0.000	0.000	-0.019
			Disease	100.000	0.019	0.019	0.000	0.000	0.000	-0.010
	Periodontitis	16	Healthy	100.000	0.036	0.036	0.000	0.000	0.000	-0.019
			PB	99.899	0.067	0.044	0.002	-12.865	494.500	-0.023
			PnB	99.894	0.068	0.045	0.002	-12.576	472.500	-0.023
		17	Healthy	99.999	0.008	0.005	0.000	-115.039	39700.000	-0.003
			Control	100.000	0.002	0.002	0.000	-350.019	367538.500	-0.001
			Disease	100.000	0.002	0.001	0.000	-409.198	502326.000	-0.001
	Smoking	18	Non-Smoker	99.995	0.014	0.010	0.000	-60.193	10867.500	-0.005
			Smoker	99.993	0.017	0.011	0.000	-50.379	7612.000	-0.006
		19	Non-Smoker	70.997	0.520	0.008	0.029	14.357	223.799	-0.004
			Smoker	91.622	0.202	0.006	0.008	18.791	387.874	-0.003
		20	Non-Smoker	99.029	0.108	0.020	0.003	7.964	211.591	-0.010
			Smoker	98.322	0.121	0.013	0.004	15.895	348.415	-0.007

Skin	Psoriasis	21	Control	96.188	0.133	0.002	0.003	38.406	1640.442	-0.001
			Normal	94.728	0.170	0.002	0.003	39.778	1789.015	-0.001
			Lesion	94.563	0.149	0.002	0.003	34.358	1341.691	-0.001
Lung	Cystic Fibrosis	22	Treated	100.000	1.000	1.000	NA	NA	NA	-1.000
			Exacerbation	100.000	0.250	0.250	0.000	0.000	0.000	-0.143
		23	Healthy	100.000	0.069	0.069	0.000	0.000	0.000	-0.036
			Disease	99.770	0.100	0.067	0.004	-8.544	217.000	-0.034
	HIV	24	Negative	13.101	0.946	0.001	0.020	29.803	1053.016	-0.001
			Positive	92.261	0.365	0.003	0.004	52.143	4337.595	-0.001
Vaginal	BV	25	Healthy	99.265	0.176	0.118	0.012	-4.814	67.500	-0.062
			BV	100.000	0.500	0.500	0.000	0.000	0.000	-0.333
Semen	Infertile (Genus level)	26	Normal	99.474	0.150	0.100	0.009	-5.672	94.500	-0.053
			Subnormal	100.000	0.091	0.091	0.000	0.000	0.000	-0.048
			Abnormal	100.000	0.071	0.071	0.000	0.000	0.000	-0.037
	Infertile (Species level)		Normal	99.993	0.012	0.002	0.000	105.660	33899.677	-0.001
			Subnormal	99.997	0.007	0.002	0.000	112.384	35971.995	-0.001
			Abnormal	99.998	0.006	0.002	0.000	102.264	55854.225	-0.001
Healthy		**Mean**		95.506	0.126	0.049	0.003	-25.693	22119.667	-0.041
		Std. Err.		2.924	0.045	0.032	0.001	14.768	12064.204	0.032
Diseased		**Mean**		97.065	0.109	0.037	0.003	-22.651	25354.820	-0.022
		Std. Err.		1.429	0.029	0.016	0.001	15.350	14832.102	0.010

Table S13. The *observed* number of shared core nodes between the healthy (H) and diseased (D) treatments in the 25 MAD (microbiome associated disease) datasets (Related to Figs 6-7)

Microbiome	Disease	Index	Healthy	Diseased	Number of Core Nodes in Healthy	Number of Core Nodes in Diseased	Shared Core Nodes	% of Core Nodes in terms of Healthy	% of Core Nodes in terms of Diseased
Gut	IBD (Inflammatory Bowel Disease)	1	Healthy	CD	36	15	1	2.78	6.67
			Healthy	UC	36	54	1	2.78	1.85
	Obesity	3	Lean	Overweight	38	53	1	2.63	1.89
			Lean	Obesity	38	257	10	26.32	3.89
	Cancer	4	Healthy	Cancer	280	182	9	3.21	4.95
	HIV	5	Negative	Treatment	278	413	22	7.91	5.33
			Negative	Non-treatment	278	382	24	8.63	6.28
		6	Negative	Treatment	246	198	15	6.10	7.58
			Negative	Non-treatment	246	185	11	4.47	5.95
		7	Negative	Positive	175	145	22	12.57	15.17
	T1D (Lean)	8	Healthy	T1D	129	147	10	7.75	6.80
	T1D (Obesity)		Healthy	T1D	167	168	20	11.98	11.90
	Gout	9	Healthy	Gout	109	105	1	0.92	0.95
	MHE	10	Healthy	MHE	61	43	6	9.84	13.95
			Control	MHE	76	43	3	3.95	6.98
	Parkinson's Disease	11	Healthy	PD	164	386	38	23.17	9.84
	Schizophrenia	12	Healthy	Schizophrenia	271	257	30	11.07	11.67
	Autism	13	Healthy	Autism	52	79	3	5.77	3.80
			Healthy	Neurotypical	52	65	0	0.00	0.00
	Atherosclerosis	14	Healthy	Atherosclerosis	236	283	29	12.29	10.25
Oral	Atherosclerosis	15	Healthy	Atherosclerosis	12	35	0	0.00	0.00
	Periodontitis	16	Healthy	PB	14	13	1	7.14	7.69
			Healthy	PnB	14	6	0	0.00	0.00
		17	Healthy	Disease	198	728	15	7.58	2.06
			Control	Disease	628	728	0	0.00	0.00
	Smoking	18	Non-smoking	Smoking	79	67	4	5.06	5.97
		19	Non-smoking	Smoking	97	156	20	20.62	12.82
		20	Non-smoking	Smoking	21	28	0	0.00	0.00
Skin	Psoriasis	21	Control	Lesion	446	508	84	18.83	16.54
			Normal	Lesion	499	508	109	21.84	21.46
Lung	Cystic Fibrosis (CF)	22	End of Treatment	Exacerbation	2	2	0	0.00	0.00
		23	Healthy	CF	6	5	0	0.00	0.00
	HIV	24	Negative	Positive	804	338	181	22.51	53.55
Vaginal	BV	25	Healthy	BV	6	2	0	0.00	0.00
Semen	Infertile (Genus level)	26	Normal	Subnormal	5	5	1	20.00	20.00
			Normal	Abnormal	5	6	0	0.00	0.00
	Infertile Species level)		Normal	Subnormal	429	473	69	16.08	14.59
			Normal	Abnormal	429	519	67	15.62	12.91
Mean & Standard Error			**Mean**		175.32	199.66	21.24	8.41	7.98
			Standard Error		31.13	33.59	5.98	1.29	1.58

Table S14. The *observed* number of shared periphery nodes between the healthy and diseased treatments in the 25 MAD (microbiome associated disease) datasets (Related to Figs 6-7)

Microbiome	Disease	Index	Healthy	Diseased	Number of Periphery Nodes in Healthy	Number of Periphery Nodes in Diseased	Shared Periphery Nodes	% of Periphery Nodes in terms of Healthy	% of Periphery Nodes in terms of Diseased
Gut	IBD (Inflammatory Bowel Disease)	1	Healthy	CD	80	71	7	8.75	9.86
			Healthy	UC	80	103	9	11.25	8.74
	Obesity	3	Lean	Overweight	114	134	12	10.53	8.96
			Lean	Obesity	114	281	23	20.18	8.19
	Cancer	4	Healthy	Cancer	316	266	11	3.48	4.14
	HIV	5	Negative	Treatment	328	416	43	13.11	10.34
			Negative	Non-treatment	328	440	27	8.23	6.14
		6	Negative	Treatment	306	250	25	8.17	10.00
			Negative	Non-treatment	306	263	23	7.52	8.75
		7	Negative	Positive	219	189	18	8.22	9.52
	T1D (Lean)	8	Healthy	T1D	174	159	19	10.92	11.95
	T1D (Obesity)		Healthy	T1D	192	190	28	14.58	14.74
	Gout	9	Healthy	Gout	156	136	17	10.90	12.50
	MHE	10	Healthy	MHE	136	107	6	4.41	5.61
			Control	MHE	144	107	12	8.33	11.21
	Parkinson's Disease	11	Healthy	PD	218	376	40	18.35	10.64
	Schizophrenia	12	Healthy	Schizophrenia	282	302	26	9.22	8.61
	Autism	13	Healthy	Autism	105	150	9	8.57	6.00
			Healthy	Neurotypical	105	109	4	3.81	3.67
	Atherosclerosis	14	Healthy	Atherosclerosis	253	283	23	9.09	8.13
Oral	Atherosclerosis	15	Healthy	Atherosclerosis	43	68	2	4.65	2.94
	Periodontitis	16	Healthy	PB	41	32	2	4.88	6.25
			Healthy	PnB	41	38	2	4.88	5.26
		17	Healthy	Disease	201	690	14	6.97	2.03
			Control	Disease	585	690	0	0.00	0.00
	Smoking	18	Non-smoking	Smoking	130	108	13	10.00	12.04
		19	Non-smoking	Smoking	151	201	20	13.25	9.95
		20	Non-smoking	Smoking	81	121	16	19.75	13.22
Skin	Psoriasis	21	Control	Lesion	452	506	94	20.80	18.58
			Normal	Lesion	517	506	106	20.50	20.95
Lung	Cystic Fibrosis (CF)	22	End of Treatment	Exacerbation	0	6	0	NA	0.00
		23	Healthy	CF	23	25	1	4.35	4.00
	HIV	24	Negative	Positive	816	345	118	14.46	34.20
Vaginal	BV	25	Healthy	BV	11	2	0	0.00	0.00
Semen	Infertile (Genus level)	26	Normal	Subnormal	15	17	0	0.00	0.00
			Normal	Abnormal	15	22	4	26.67	18.18
	Infertile Species level)		Normal	Subnormal	428	553	63	14.72	11.39
			Normal	Abnormal	428	545	51	11.92	9.36
Mean & Standard Error			**Mean**		208.79	231.76	23.37	10.15	9.11
			Standard Error		29.40	31.41	4.65	1.02	1.06

Table S15. The *observed* number of shared skeletons with *HSS*>0 between the healthy and diseased treatments in the 25 MAD (microbiome associated disease) datasets (Related to Figs 6-7)

Microbiome	Disease	Index	Healthy	Diseased	Number of Edges in Healthy	Number of Edges Diseased	Shared Edges	% of Edges in terms of Healthy	% of Edges in terms of Diseased
Gut	IBD (Inflammatory Bowel Disease)	1	Healthy	CD	6669	3653	49	0.73	1.34
			Healthy	UC	6669	12244	80	1.20	0.65
	Obesity	3	Lean	Overweight	11470	17390	166	1.45	0.95
			Lean	Obesity	11470	105694	1132	9.87	1.07
	Cancer	4	Healthy	Cancer	177296	100128	630	0.36	0.63
	HIV	5	Negative	Treatment	183240	343199	6984	3.81	2.03
			Negative	Non-treatment	183240	337262	3762	2.05	1.12
		6	Negative	Treatment	152069	100127	2718	1.79	2.71
			Negative	Non-treatment	152069	100127	1934	1.27	1.93
		7	Negative	Positive	77417	55596	2049	2.65	3.69
	T1D (Lean)	8	Healthy	T1D	45752	46663	1059	2.31	2.27
	T1D (Obesity)		Healthy	T1D	64261	63902	3393	5.28	5.31
	Gout	9	Healthy	Gout	34962	28916	407	1.16	1.41
	MHE	10	Healthy	MHE	19306	11175	172	0.89	1.54
			Control	MHE	24089	11175	309	1.28	2.77
	Parkinson's Disease	11	Healthy	PD	64123	173070	3630	5.66	2.10
	Schizophrenia	12	Healthy	Schizophrenia	152628	155959	4861	3.18	3.12
	Autism	13	Healthy	Autism	12245	23827	43	0.35	0.18
			Healthy	Neurotypical	12245	15043	24	0.20	0.16
	Atherosclerosis	14	Healthy	Atherosclerosis	119315	159894	4288	3.59	2.68
Oral	Atherosclerosis	15	Healthy	Atherosclerosis	1485	5253	2	0.13	0.04
	Periodontitis	16	Healthy	PB	1485	989	1	0.07	0.10
			Healthy	PnB	1485	945	1	0.07	0.11
		17	Healthy	Disease	79400	1004652	1353	1.70	0.13
			Control	Disease	735077	1004652	0	0.00	0.00
	Smoking	18	Non-smoking	Smoking	21735	15224	279	1.28	1.83
		19	Non-smoking	Smoking	21745	58222	1707	7.85	2.93
		20	Non-smoking	Smoking	5101	10841	153	3.00	1.41
Skin	Psoriasis	21	Control	Lesion	387400	485669	37098	9.58	7.64
			Normal	Lesion	488439	485669	64145	13.13	13.21
Lung	Cystic Fibrosis (CF)	22	End of Treatment	Exacerbation	1	28	0	0.00	0.00
		23	Healthy	CF	406	434	0	0.00	0.00
	HIV	24	Negative	Positive	171801	214879	19746	11.49	9.19
Vaginal	BV	25	Healthy	BV	135	6	0	0.00	0.00
Semen	Infertile (Genus level)	26	Normal	Subnormal	189	231	3	1.59	1.30
			Normal	Abnormal	189	378	6	3.17	1.59
	Infertile Species level)		Normal	Subnormal	366772	525807	26291	7.17	5.00
			Normal	Abnormal	366772	565507	24225	6.60	4.28
Mean & Standard Error			**Mean**		109477.68	164327.1	5597.37	3.05	2.27
			Standard Error		26413.27	41954.41	2086.53	0.57	0.45

Supplementary Figs S1-S3

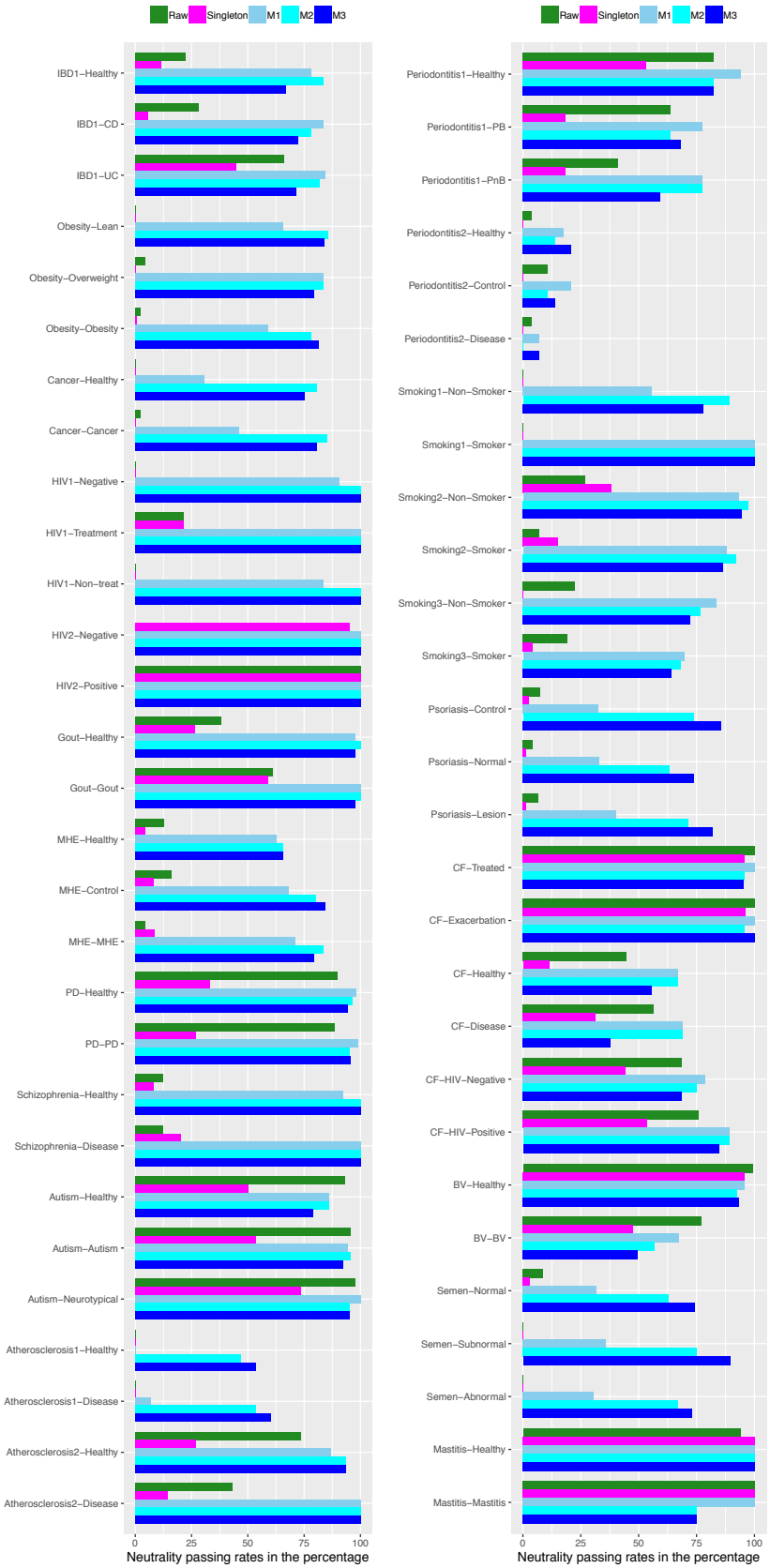

Fig S1. The neutrality passing rates for each of the 24 case studies: for each case, the test results for five data pre-processing schemes are plotted (Related to Fig 2).

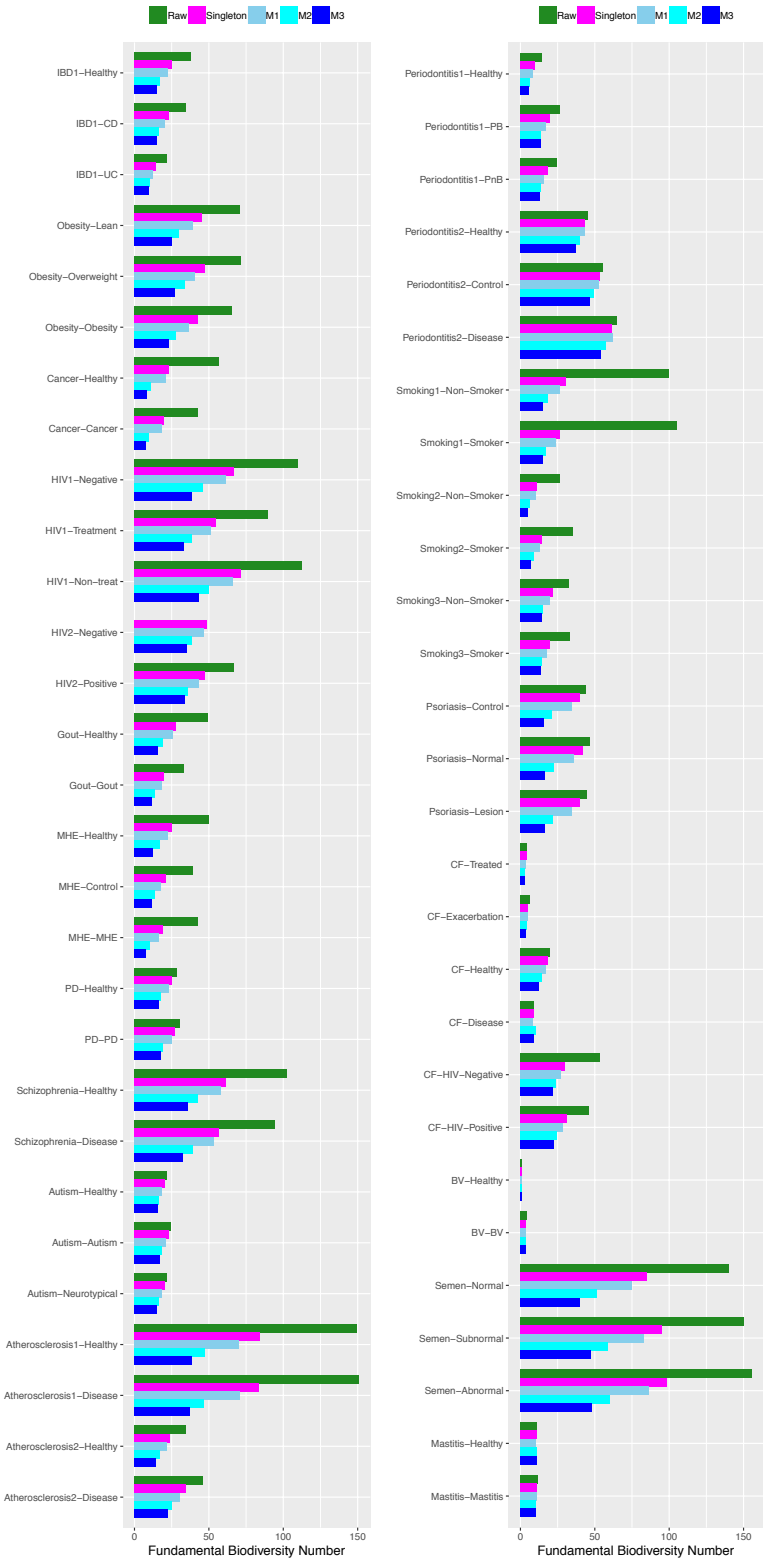

Fig S2. The fundamental diversity number (θ) for each of the 24 case studies: for each case study, the test results for five data pre-processing schemes are plotted (Related to Fig 3).

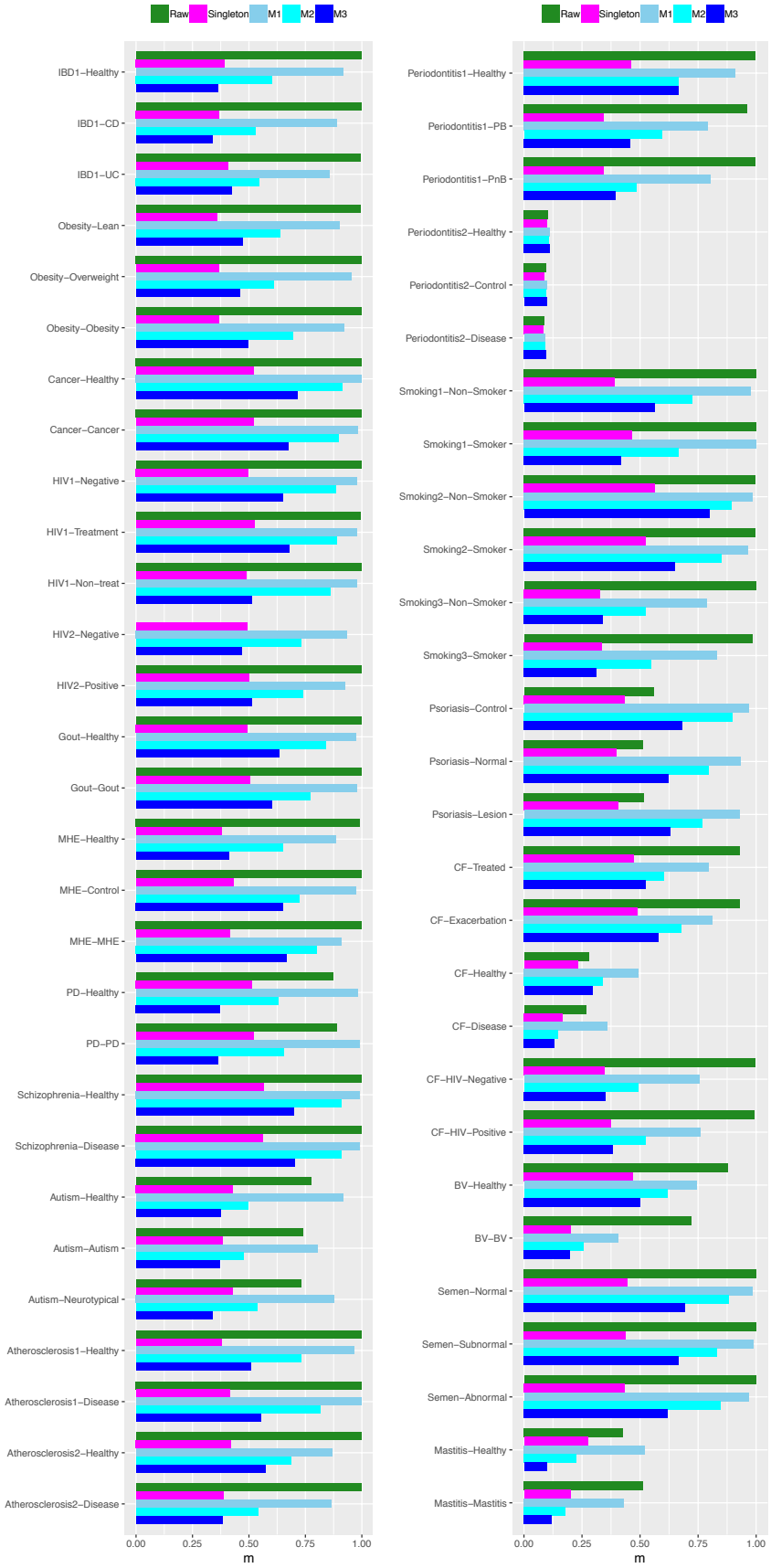

Fig S3. The immigration probability (*m*) (fundamental dispersal number) for each of the 24 case studies, for each case study, the test results for five data pre-processing schemes are plotted (Related to Fig 3).

Transparent Methods

Datasets of Human Microbiome Associated Diseases

A brief description on the metagenomic datasets of the 27 MAD (microbiome associated disease) studies is provided in Table S1 of the online supplementary information (OSI), which are the same datasets used in Ma *et al*. (2019). Among the 27 datasets, there were 3 and 2 datasets that are not suitable for the neutral-theoretic analysis and CPN/HSN analyses, respectively, and therefore were excluded from the analyses of this study. The 27 case studies cover most of the high-profile MAD including obesity, IBD, diabetes, BV (bacterial vaginosis), periodontitis, and neurodegenerative diseases. The datasets were in the abundance of 16s-rRNA reads clustered at the species level (97% similarity level), equivalent with the species abundance tables in macrobial ecology.

Hubbell's unified neutral theory of biodiversity (UNTB)

Hubbell (2001) classic neutral theory describes a local community containing J individuals, one of which, randomly chosen, dies and is replaced at every time step. Two ways the individual is replaced are: an offspring of another randomly chosen individual from the local community, occurring with probability $(1–m)$, or offspring from a randomly chosen individual from an outside pool of individuals (metacommunity) with probability m. The metacommunity is a well-mixed source pool of individual organisms; each individual has the potential to reproduce offspring migrated to the local community being studied. Neutral theory assumes that the species abundance distribution (SAD) of metacommunity is governed by a similar neutral process. The replacement individuals in the metacommunity are offspring from a randomly chosen individual in the metacommunity, or from speciation (which occurs with probability v). Obviously, in previous description of community dynamics (birth, death, migration, speciation), all individuals are assumed to be equivalent and are distinguished only by their species labels. The species labels are preserved solely for describing SAD.

The neutral theory is formulated as a sampling theory, which takes into account the effect of sampling a small proportion from the much larger natural system (sampling space). The mathematical model used to describe the neutral process is multi-nominal distribution, which can be mechanistically derived from a master equation—a differential equation that describes the community dynamics based on the neutral principles. It makes predictions about SADs, which can be statistically tested against observed species abundances data obtained from sampling actual communities. In the following, we briefly describe the parameters and statistical tests used in testing the neutrality for a sole purpose to interpret the results from our analysis.

The total number of individuals of all species in a local community (represented as $\boldsymbol{J}$) is the local community size. In our case, it is the total number of 16s-rRNA reads of all OTUs from a community sample. The UNTB assumes a finite community size.

The number of species ($\boldsymbol{S}$) in the community may change due to speciation, extinction and immigration from meta-community.

The fundamental biodiversity number (θ) is actually a measure of speciation, which can be seen from its definition, $\theta = J_M[v/(1-v)]$, where J_M is the number of individuals in the metacommunity and v is the per capita speciation rate. Therefore, the fundamental biodiversity number (θ) represents the speciation process in Vellend (2010) & Hanson et al. (2012) synthesis for community patterns.

The immigration probability (m) is a measure for *dispersal limitation*, and it is defined as $m=I/(I+J-1)$, where I is the number of immigrants that are searching for vacant spot in the local community (*i.e*., competing with the local individuals), and J is the number of individuals as mentioned previously. Dispersal limitation is a process that causes the location of an individual to be limited in some sense by the location of its parent (Rosindell *et al*. 2011). The immigration probability (m) therefore, characterizes the dispersal process in Vellend (2010) and Hanson *et al.* (2012) synthesis for community ecology.

Etienne's (2005, 2007) exact neutrality test adopts a mixture test strategy of Monte Carlo (simulation) significance test and the parametric bootstrap. The test is 'exact' since type I error can be *exactly* specified. It compares the probability (the likelihood) of the realized or observed configuration (*i.e*., SAD of actually sampled community) with the probabilities of the artificially simulated configurations based on the neutral theory model by using a Chi-squared test. If the p-value from the test is $p>0.05$, we conclude that the neutrality of the community under testing cannot be rejected, and that the observed SAD is consistent with the prediction from the neutral theory, *i.e.,* passing the neutrality test.

To apply Hubbell's (2001) UNTB for measuring the effects of drift, speciation and dispersal (Rosindell *et al*. 2011), we adopted Etienne (2005) sampling formula (distribution model) and a standard *R*-package UNTB by Hankin (2007) that implemented Etienne (2005) exact probability test procedure. An illustration of testing the neutrality of the human microbiome is provided in Li & Ma (2015).

In consideration of the potential influence of sequencing errors on the neutrality test, we removed singleton (removing the OTUs represented by a single read), minus one, two, and three reads across all OTUs, respectively. We also included the test with "raw" OTU reads, *i.e*., without removing any reads from the OTU tables computed from standard bioinformatics pipelines used in Ma *et al*. (2019). That is, a total of five tests are performed for each community sample based on five different data pre-processing schemes to enhance the robustness of our analysis.

Fisher's exact probability test is designed to compare the frequency of occurrences (observations) in a fourfold table setting when the numbers are too small to use the Chi-square test (Fisher 1922, 1954). We use Fisher's exact probability test to determine if there are pair-wise differences between the treatments (the healthy and diseased) in their passing rates of the neutrality test. We used the *R*-function (fisher.test) from the standard R-package (stats) (http://stat.ethz.ch/R-manual/R-patched/library/stats/html/fisher.test.html) to conduct the Fisher's exact test in this study. Note that the step of Fisher's exact test was performed after the FDR (false discovery rate, *i.e*., multiple testing corrections) control for the p-values from Etienne's (2005) neutrality test of Hubbell's (2001) UNTB.

Ning et al. (2019) framework for quantifying ecological stochasticity

We use a new framework recently developed by Ning *et al*. (2019) for quantifying ecological stochasticity to cross-verify the results from neutral theory modeling. The theoretical basis of their mathematical framework is that deterministic processes should drive ecological communities more similar or dissimilar than null expectation, and they formulated a sophisticated procedure to implement a null model for quantifying stochasticity. Our motivation to apply Ning *et al*. (2019) framework for estimating community stochasticity level is to cross-verify the findings from Hubbell's UNTB, especially to determine a possible ceiling limit for stochasticity given that UNTB model tended to overestimate the stochastic neutral processes.

Technically, this is possible since the normalized stochasticity ratio (NSR) of Ning *et al.* (2019) is a dimensionless metric in percentages or between *0* and *1*. The *NSR* represents for the *strength of stochasticity* in the community assembly, and should range from 0 to 100%. If the community assembly is extremely deterministic without any stochasticity, then *NSR* should be 0%; otherwise *SR* should be 100%. However, when expected stochasticity is very low, *NSR* could overestimate stochasticity (Ning *et al*. 2019).

Core/periphery network (CPN)

Given that network analysis has been widely applied to microbiome research (*e.g.,* Faust *et al*. 2012, Faust & Raes 2012, Kurtz *et al*. 2015, Ma & Ye 2017, Xiao *et al*. 2017, Röttjers & Faust 2018, Ma & Ellison 2019), what are special with CPN or HSN (*see* next sub-section)? Informally, the network core usually denotes a centrally and densely connected set of network nodes, while the network periphery refers to a sparsely connected, usually non-central set of nodes that are linked to the core (Csermely *et al*. 2013). Ecological communities/systems are typical complex systems (networks), which can be formulated as core/periphery network (CPN). More recent studies established that network cores promotes system robustness and evolvability, which can help system to adapt to large fluctuations of the environment, as well as to noise of intrinsic processes (Csermely *et al*. 2013). The core/periphery structure was found to be ubiquitous in the species dominance network of the human vaginal microbiome and the structure plays an important role in controlling the community diversity-stability relationships (Ma & Ellison 2019). For example, an extensive core (extensively large core size) allows for a more resilient network (community) but could be more difficult to control.

According to Csermely *et al*. (2013), a perfect or ideal core/periphery network consists of a fully linked core and a periphery that is fully connected to the core, but none of the periphery nodes are connected with each other. Formally, let $G=(V, E)$ be an undirected, unweighted graph with n nodes and m edges, and let $A=(a_{ij})$ is the adjacency matrix of G, where $a_{ij}=1$ if node i & node j are linked and *0* otherwise. Let δ be a vector of length n with entries of *1* or *0*, if the corresponding node belongs to the core or the periphery, respectively. Additionally, let $P=(p_{ij})$ be the adjacency matrix of the ideal or perfect core/periphery network of n nodes and m edges. The detection of core-periphery structure is an optimization problem to find the vector δ such that the objective function (ρ) achieves its maximum. With the vector δ, it is then trivial to classify nodes into either core or periphery.

$$\rho = \sum_{i,j} A_{ij} P_{ij} \qquad (1)$$

When applied to the human microbiome, the CPN structures reflect the heterogeneity or asymmetry of species (OTUs) from node perspective. In terms of the Vellend-Hanson four-processes synthesis (Vellend 2010, Hanson et al. 2012), which states that drift, speciation, dispersal, and selection are the underlying processes or mechanisms shaping community diversity patterns and driving community dynamics, the heterogeneity or asymmetry of species (nodes) revealed by CPN represents for the effects of *selection.* Therefore, at least, conceptually, the CPN analysis offers a framework to investigate the effects of selection from node perspective.

More importantly, the core/periphery (nodes or species) can be considered as critical network structures, and we postulate that they should be more sensitive to disturbances including MADs. In the present study, we mainly perform two kinds of statistical tests with CPNs. The first is to conduct shared core/periphery analysis, which assesses and interprets the effects of MADs on the possible increase or decrease of shared core/periphery between the healthy and diseased

individuals. The second is to test the differences between the healthy and diseased individuals in the properties of critical network structures.

High-salience skeleton network (HSN) and network assortativity

While core/periphery network distinguishes the different structural and functional roles between core and periphery nodes (species), the high-salience skeleton network (HSN) makes distinctions among the links (edges). Arguably the most important reason (also the advantage) why network analysis has been experiencing explosion is its capacity in reducing the *complexity* of complex systems (networks) while preserving their certain key features. In other words, network analysis can shed critical lights on complex networks by reducing complexity and leveraging the information from the key features. The HSN allows us to focus on critical paths (interactions) in complex networks (Grady *et al*. 2012, Shekhtman *et al*. 2014).

High salience skeletons or backbones reduce the number of links in the network while preserving the nodes (Grady *et al*. 2012, Shekhtman *et al*. 2014). However, reducing link complexity is particularly challenging because of the *mix* of link and node heterogeneity. In the case of human microbiome network, the heterogeneities of both nodes and links were equally significant, which is evidenced by the near universal fitting of the power law distributions to various network properties of nodes and links (Ma & Ellison 2019). Whether generic heterogeneous networks can be intrinsically segregated into qualitatively distinct clusters is still an open problem in network theory (Grady *et al*. 2012, Shekhtman *et al*. 2014). Grady *et al*. (2012) introduced the concept of link salience to deal with the problem, which measures the significance of a link and is based on an ensemble of node-specific perspectives of the network, and quantifies the extent to which a consensus among nodes exist regarding the importance of a link. The so-termed *high-salience skeletons* then constitute the backbones ("highways") of the network.

Besides identifying backbones or highways in complex networks, another advantage of high salience skeleton network is its particular suitability for exploring the response of networks under different perturbations such as intentional attack and random failure. High salience network has been particularly successful in the studies of transportation networks, where skeletons (backbones) are responsible for carrying the majority of the traffic. When encountering perturbations such as traffic jams or natural disasters, backbones again are critical for transportation rerouting and cancellations to survive disasters (Grady *et al*. 2012, Shekhtman *et al*. 2014). In this study, MADs can be treated as perturbations at ecological time scale and as selection force at evolutionary time scale, which may not be separable according to Hanson *et al*. (2012) due to the fast-track evolution of microbes.

Link salience (s) is defined based on the notion of shortest paths in weighted networks, *e.g*., the species correlation network with the *inverse* of correlation coefficients as weights (Ma & Ellison 2019). Assume a weighted network defined by weight matrix w_{ij} and a shortest path between node x and y, the indicator function can be defined as: $\sigma_{ij}(y, x) = 1$ if edge (i, j) is on the shortest path from x to y, $\sigma_{ij}(y, x) = 0$, otherwise. A shortest path tree $T(x)$ rooted at node x is described by a matrix with elements: $T_{ij}(x) = 1$, if $\sum_{y} \sigma_{ij}(y, x) > 0$, $T_{ij}(x) = 0$ otherwise. Link salience s_{ij} of edge (i, j) is computed with the following formula:

$$s_{ij} = \frac{1}{N} \sum_{x} T_{ij}(x) = \left\langle T_{ij}(x) \right\rangle_{V} \qquad (2)$$

where $\langle \bullet \rangle_{V}$ is the average across the set of root nodes x.

As explained previously, when applied to the human microbiome, the high salience skeletons (links) reflect the heterogeneity or asymmetry of species (OTUs) interactions from the link perspective. According to the four-process synthesis (Vellend 2010, Hanson *et al*. 2012), heterogeneity or asymmetry of species interactions or species interactions with their environments represents for the effects of *selection,* which can be revealed by the HSN introduced here from link perspective, cross-verified with the CPN from node perspective introduced previously.

Specifically, we will first test whether or not the *shared* high-salience skeletons between the healthy and diseased individuals are increased or decreased due to the disease effects, similar to the previously described shared core/periphery nodes analysis. Second, we will also test the properties of high-salience skeleton networks, which are critical network structures from link perspective, similar to the testing of properties of core/periphery network from node perspective. Furthermore, integrated with previous CPN analysis, the combined *shared analyses* of the core/periphery/skeleton structures, as well as testing the differences in the key properties of the core/periphery/skeleton networks, are expected to reveal the differences between the healthy and diseased individuals and identify potentially invaluable diagnosis and risk prediction indicators for MADs.

As to the CPN/HSN properties, we mention one particularly important network property, the *assortativity* coefficient. The property is important because it is highly relevant to network resilience, the loss of which is known as *dysbiosis* in the literature of human MADs. In assortative networks, the nodes with many connections tend to be connected to other nodes that also possess many connections (Newman 2002, 2003). The assortativity coefficient (r) is a concept for measuring the homophyly level of the graph (network). The homophyly refers to resemblance due to common ancestry based on values (such as degree) assigned to vertices. A higher assortativity coefficient (r) indicates that connected vertices tend to have more similar assigned values. For an undirected network, the assortativity based on vertex degree is defined as

$$r = \frac{1}{\sigma_q^2} \sum_{jk} jk(e_{jk} - q_j q_k), \qquad (3)$$

where e_{jk} is the fraction of edges connecting vertices of type j and k (*i.e.*, vertices that have degrees j and k), σ_q is the standard deviation of the distribution q_k, and q_k is equal to: $q_k = \sum_j e_{jk}$.

From eqn. (3), one can find that the r is equal to the Pearson's correlation coefficient of degree between pairs of linked nodes. The value of r lies in the range $-1 \le r \le 1$, with $r = 1$ indicating perfect assortativity and $r = -1$ indicating perfect disassortativity. When the value of r lies around 0, it is null or neural result, meaning that it is not statistically different from zero. Assortative networks are more resilient against removal of their vertices, especially highest-degree vertices, than disassortative or neutral ($r \approx 0$) networks. The above definition for assortativity index is based on general complex network such as species correlation network (SCN). In this study, we compute the assortativity (r_{HSS}) for the high-salience skeleton networks based on the degree of high-salience skeletons (HSS) of vertices. Different from SCNs, the high-salience skeleton networks are typically disassortative (Grady 2012).

Computational procedures/algorithms for CPN & HSN analyses

As introduced previously, two types of statistical tests, *i.e*., the shared core/periphery/skeleton analyses between the healthy (H) and diseased (D) treatments (*i.e.,* test the change of shared critical network structures between the H & D treatments), as well as test the differences in key properties of the critical network structures between the H & D treatments. Both types of tests depend on the construction of CPN/HSN, which are built from species correlation networks

(SCN). The samples from both H & D treatments are randomly mixed before building SCN networks. From the randomly mixed (permutated) samples, 1000 pairs (pair=H *vs*. D) of permutated networks are constructed, and the *p*-values of the permutation tests for determining the significances of the differences (*i.e*., disease effects) are computed from comparing the 1000 pairs of networks. Spearman's correlation coefficients with FDR (false discovery rate) control with *p*-value=0.001 are first used to construct SCNs. From the SCNs, the algorithms outlined in previous sections are applied to reconstruct the corresponding CPN and HSN networks. The computation procedures for building SCN can be found in Junker & Schreiber (2008) and Ma & Ye (2017), and those for building CPN/HSN can be found in Ma & Ellison (2019). Further information on the algorithms for performing the two types of statistical tests outline above is briefly introduced below:

General outline for generating permutated networks for performing shared core/periphery/skeleton analyses and for testing the network properties

(1) Building 1000 sets (pairs) of healthy (*H*) & diseased (*D*) networks by randomly reshuffling the *H* and *D* samples for 1000 times using Spearman's rank correlation coefficients with FDR (false discovery control).

A. For Shared Core/Periphery (Nodes) Analysis
(2A) Detect core/periphery nodes from the *H* & *D* networks built in (*1*), construct core/periphery networks (CPN), and compute shared core/periphery nodes between the *H* & *D* samples.
(3A) Perform permutation test with the 1000 permutated networks and test the change of shared core/periphery nodes between the *H* & *D* samples, based on the results from (*2A*).

B. For Shared Skeleton (Edge or Link) Analysis
(2B) Detect high salience skeletons from the H & D networks built in (*1*), construct high salience skeleton networks (HSN), and compute the shared skeletons between the H & D samples.
(3B) Perform permutation test with the 1000 permutated networks and test the change of shared skeletons between the H & D samples, based on the results from (*2B*).

C. Significance Test for Core/Periphery and Skeleton Networks Properties
Using the results from A & B to test the difference in the network properties by performing the standard permutation tests.

Test Algorithms

Algorithm for Shared Core/Periphery Analysis based on Permutated Networks
Step [1]: Assuming there are *a* samples from the healthy (*H*) treatment, and *b* samples from the diseased (*D*) treatment, compute the pair-wise Spearman's correlation coefficients for the *a* samples in the H and the *b* samples in the *D* treatment, respectively. Use FDR control with *p*=0.001 to filter out insignificant correlations, and obtain the final correlation relationships for building the species correlation networks for the *H* and *D* treatments. From the two species correlation networks, detect the core/periphery nodes for each network, and compute the shared core/periphery nodes between the *H* & *D* networks, respectively. This step is no difference from regular core/periphery network analysis, until computing the shared core/periphery nodes.

The shard core/periphery nodes obtained from this *Step* [1] is the actually or *observed* shared core/periphery nodes.

Step [2]: Pool together all samples from *H* & *D* and perform random permutation of the combined (*a*+*b*) samples. Treat the first *a* samples as the permutated healthy treatment and the leftover *b* samples as the permutated diseased treatment.

According to the algorithm in *Step* [1], compute the shared core/periphery nodes for this specific pair of permutated *H* & *D* treatments.

Step [3]: Repeat *Step* [2] for 1000 times, and obtain 1000 sets of shared core/periphery nodes.

Step [4]: Compute a pseudo-*p* value. Using the number of shared core nodes as example, assume the shared core nodes from **Step [1]** is *N*, the numbers of shared core nodes from the 1000 random permutations in *Step* [2-3] are $N_1, N_{2,...,} N_{i,...}N_{1000}$, the pseudo-*p* value is the proportion of the permutations with $N_i>N$ among 1000 times of permutations. That is, assuming *n* is the number of times satisfying $N_i>N$ in 1000 permutations, $p=n/1000$.

Algorithm for Shared Skeleton Analysis Based on Permutated Networks
Step [1]: Assuming there are *a* samples from the healthy (*H*) treatment, and *b* samples from the diseased (*D*) treatment, compute the pair-wise Spearman's correlation coefficients for the *a* samples in the H and the *b* samples in the *D* treatment, respectively. Use FDR control with $p=0.001$ to filter out insignificant correlations, and obtain the final correlation relationships for building the species correlation networks for the *H* and *D* treatments. From the two species correlation networks, compute the HSS (high salient skeleton) value for each edge, and compute the shared skeletons between the *H* & *D* networks with HSS>0, and HSS≥0.2, respectively. This step is no difference from regular skeleton network analysis, until computing the shared skeletons.

The shard skeletons obtained from this *Step* [1] is the actually or *observed* shared skeletons.

Step [2]: Pool together all samples from *H* & *D* and perform random permutation of the combined (*a*+*b*) samples. Treat the first *a* samples as the permutated healthy treatment and the leftover *b* samples as the permutated diseased treatment.

According to the algorithm in *Step* [1], compute the shared skeletons for this specific pair of permutated *H* & *D* treatments.

Step [3]: Repeat *Step* [2] for 1000 times, and obtain 1000 sets of shared skeletons.

Step [4]: Compute a pseudo-*p* value. Assume the shared skeletons from **Step [1]** is *N*, the numbers of shared skeletons from the 1000 random permutations in Step [2-3] are $N_1, N_{2,...,} N_{i,...}N_{1000}$, the pseudo-*p* value is the proportion of the permutations with $N_i>N$ among 1000 times of permutations. That is, assuming *n* is the number of times satisfying $N_i>N$ in 1000 permutations, $p=n/1000$.

References (Cited in "Transparent Methods")

Abusleme L, Dupuy AK, Dutzan N, et al. (2013) The subgingival microbiome in health and periodontitis and its relationship with community biomass and inflammation. *The ISME Journal*, 7(5):1016-1025.

Alekseyenko AV, Perezperez GI, Souza AD, et al. (2013) Community differentiation of the cutaneous microbiota in psoriasis. *Microbiome*,1,1(2013-12-23), 1(1):31-31.

Blainey PC, Milla CE, Cornfield DN, et al. (2012) Quantitative analysis of the human airway microbial ecology reveals a pervasive signature for cystic fibrosis. *Science Translational Medicine*, 4(153):153ra130.

Charlson ES, Chen J, Custersallen R, et al. (2010). Disordered microbial communities in the upper respiratory tract of cigarette smokers. *Plos One*, 5(12):e15216.

Csermely P, London A, Wu LY, Uzzi B. Structure and dynamics of core/periphery networks. *Journal of Complex Networks.* 2013;1:93-123.

Dilip V. Jeste (UC San Diego) https://profiles.ucsd.edu/dilip.jeste

Etienne RS (2005) A new sampling formula for neutral biodiversity. *Ecology Letters* 8(3):253-260.

Etienne RS. (2007) A neutral sampling formula for multiple samples and an 'exact' test of neutrality. *Ecology Letters* 10(7): 608-618.

Faust K, Sathirapongsasuti JF, Izard J, Segata N, Gevers D, Raes J et al. (2012) Microbial co-occurrence relationships in the human microbiome. *PLoS Comput Biol*. 2012;8(7):e1002606.

Faust K, Raes J. (2012) Microbial interactions: from networks to models. *Nat Rev Microbiol*. 10:538–550.

Fisher RA (1922) On the interpretation of χ^2 from contingency tables, and the calculation of p-value. *Journal of the Royal Statistical Society*. Vol. 85(1): 87–94.

Fisher RA (1954) Statistical Methods for Research Workers. *Oliver and Boyd*. ISBN 0-05-002170-2.

Fodor AA, Klem ER, Gilpin DF, et al. (2012) The Adult Cystic Fibrosis Airway Microbiota Is Stable over Time and Infection Type, and Highly Resilient to Antibiotic Treatment of Exacerbations. *Plos One*, 7(9):e45001.

Grady D, Thiemann C, Brockmann D. (2012) Robust classification of salient links in complex networks. *Nature Communications.* 2012;DOI: 10.1038/ncomms1847

Griffen AL, Beall CJ, Campbell JH, et al. (2012) Distinct and complex bacterial profiles in human periodontitis and health revealed by 16S pyrosequencing. *The ISME Journal*, 6(6):1176.13

Guo Z, Zhang J, Wang Z, et al. (2016) Intestinal Microbiota Distinguish Gout Patients from Healthy Humans. Sci Rep, 6:20602.

Halfvarson J, Brislawn CJ, Lamendella R, et al. (2017) Dynamics of the human gut microbiome in Inflammatory Bowel Disease. *Nature Microbiology*, 2:17004.

Hankin RKS (2007) Introducing UNTB, an R Package For Simulating Ecological Drift Under the Unified Neutral Theory of Biodiversity. *Journal of Statistical Software*. 22(12):15pp. (https://cran.r project.org/web/packages/untb/index.html)

Hanson CA, Fuhrman JA, Horner-Devine MC, Martiny JBH (2012) Beyond biogeographic patterns: processes shaping the microbial landscape. *Nat Rev Microbiol*. Vol.10:497–506

Hill-Burns EM, Debelius JW, Morton JT et al. (2017) Parkinson's Disease and PD Medications Have Distinct Signatures of the Gut Microbiome. *Movement Disorders Official Journal of the Movement Disorder Society*, 32(5):739.

Hubbell SP (2001) The unified neutral theory of biodiversity and biogeography. *Princeton University Press*.

Junker BH, Schreiber F. (2008) *Analysis of biological networks*. Wiley. 2008.

Kang DW, Adams JB, Gregory AC, et al. (2017) Microbiota Transfer Therapy alters gut ecosystem and improves gastrointestinal and autism symptoms: an open-label study. *Microbiome*, 5(1):10

Kim, Jane (https://clinicaltrials.gov/ct2/show/NCT02938806)

Koren O, Klaenhammer TR. (2011) Human oral, gut, and plaque microbiota in patients with atherosclerosis. *PNAS*, 108(Suppl 1):4592-4598.

Kurtz ZD, Müller CL, Miraldi ER, Littman DR, Blaser MJ, Bonneau RA. (2015) Sparse and Compositionally Robust Inference of Microbial Ecological Networks. *PLOS Comp. Biol*. 2015. https://doi.org/10.1371/journal.pcbi.1004226

Lazarevic V, Whiteson K, Hernandez D, et al. (2010) Study of inter- and intra-individual variations in the salivary microbiota. *BMC Genomics*, 11(1):1-11.

Li LW, Ma ZS (2016) Testing the Neutral Theory of Biodiversity with Human Microbiome Datasets. *Scientific Reports*. 2016;6, Article No. 31448

Lozupone C, Cota-Gomez A, Palmer B E, et al. (2013) Widespread colonization of the lung by Tropheryma whipplei in HIV infection. *American Journal of Respiratory & Critical Care Medicin*e, 187(10):1110-1117.

Ma ZS, Ye D. (2017) Trios—promising *in silico* biomarkers for differentiating the effect of disease on the human microbiome network. *Sci Rep* 2017;**7**:13259.

Ma ZS, Ellison AM (2019) Dominance network analysis provides a new framework for studying the diversity-stability relationship. *Ecological Monographs*. https://esajournals.onlinelibrary.wiley.com/doi/full/10.1002/ecm.1358

Ma ZS, Li LW, Gotelli NJ (2019) Diversity-disease relationships and shared species analyses for human microbiome-associated diseases, *The ISME Journal*. 2019;DOI: 10.1038/s41396-019-0395-y

Mchardy IH, Li X, Tong M, et al. (2013) HIV Infection is associated wth compositional and functional shifts in the rectal mucosal microbiota. *Microbiome*, 1(1):26.

Neff CP, Krueger O, Xiong K, et al. (2018) Fecal Microbiota Composition Drives Immune Activation in HIV-infected Individuals. *Ebiomedicine*, 30

Newman, MEJ (2002) Assortative mixing in networks. *Physical Review Letters*, 89(20), 208701.

Newman MEJ (2003) Mixing patterns in networks. *Phys. Rev. E* 67, 026126

Ning D, Deng Y, Tiedje JM, Zhou J (2019) A general framework for quantitatively assessing ecological stochasticity. *PNAS*, 116 (34): 16892-16898.

Papa E, Docktor M, Smillie C, et al. (2012) Non-Invasive Mapping of the Gastrointestinal Microbiota Identifies Children with Inflammatory Bowel Disease. *Plos One*, 7(6):e39242.

Rosindell J, Hubbell SP, Etienne RS. (2011) The Unified Neutral Theory of Biodiversity and Biogeography at Age Ten. *Trends in Ecology & Evolution.* Vol. **26**:340–348.

Röttjers L, Faust K (2018) From hairballs to hypotheses–biological insights from microbial networks. *FEMS Microbiology Reviews*, 42(6):761–780. https://doi.org/10.1093/femsre/fuy030

Shekhtman LM, Bagrow JP, Brockmann D. (2014) Robustness of skeletons and salient features in networks. *Journal of Complex Networks*. doi:10.1093/comnet/cnt019

Srinivasan S, Hoffman NG, Morgan MT, et al. (2012) Bacterial Communities in Women with

Bacterial Vaginosis: High Resolution Phylogenetic Analyses Reveal Relationships of Microbiota to Clinical Criteria. *Plos One*, 7(6):e37818.

Turnbaugh PJ, Hamady M, Yatsunenko T, et al. (2009) A core gut microbiome in obese and lean twins. *Nature*, 457(7228):480.

Urbaniak C, Mcmillan A, Angelini M, et al. (2014) Effect of chemotherapy on the microbiota and metabolome of human milk, a case report. *Microbiome*, 2(1):24.

Vellend M (2010) Conceptual synthesis in community ecology. *Q. Rev. Biol*. 2010;85:183–206

Wang T, Cai G, Qiu Y, et al. (2012) Structural segregation of gut microbiota between colorectal cancer patients and healthy volunteers. ,*The ISME Journal* 6(2):320-329.

Weng SL, Chiu CM, Lin FM, et al. (2014) Bacterial Communities in Semen from Men of Infertile Couples: Metagenomic Sequencing Reveals Relationships of Seminal Microbiota to Semen Quality. *Plos One*, 9(10):e110152.

Xiao Y, Angulo MT, Friedman J, Waldor MK, Weiss ST, Liu YY. (2017) Mapping the ecological networks of microbial communities. *Nature Communications*. Vol. **8**, Article number: 2042

Zhang Z, Zhai H, Geng J, et al. (2013) Large-scale survey of gut microbiota associated with MHE Via 16S rRNA-based pyrosequencing. *American Journal of Gastroenterology*, 108(10):1601-1611.